Masterarbeit

Design, Construction and Characterization of a Tungsten Boat Furnace

Paul Tirk, BSc

Institut für Analytische Chemie und Lebensmittelchemie
Technische Universität Graz

Betreuer: Dr. techn. Dipl.-Ing. Helmar Wiltsche

Graz, im Mai 2012

Statutory Declaration

I declare that I have authored this thesis independently, that I have not used other than the declared sources / resources, and that I have explicitly marked all material which has been quoted either literally or by content from the used sources.

Eidesstattliche Erklärung

Ich erkläre an Eides statt, dass ich die vorliegende Arbeit selbstständig verfasst, andere als die angegebenen Quellen/Hilfsmittel nicht benutzt, und die den benutzten Quellen wörtlich und inhaltlich entnommenen Stellen als solche kenntlich gemacht habe.

Graz, am _____ _____

Unterschrift

"Heavy metal is our business."

Danksagung

Ich möchte mich im Rahmen dieser Masterarbeit – und damit meines bevorstehenden Studienabschlusses – bei folgenden Personen besonders bedanken:

Bei meinen Eltern, die es mir überhaupt ermöglicht haben, studieren zu können, auf eigenen Beinen zu stehen und mich persönlich zu entfalten.

Bei meinen Freunden, die mir in dieser Zeit immer und überall zur Seite standen und mich mit Ratschlägen und ermutigenden Worten bedachten.

Bei all meinen Kollegen, denen ich ein absolut angenehmes und freundschaftliches Arbeitsklima verdanke.

Und zuletzt natürlich bei meinem Betreuer, Helmar Wiltsche, ohne den diese Arbeit nie zustande gekommen wäre und der für jede interessante – und sei es auch ein bisschen „verrückte“ – Idee zu begeistern war, sowie bei allen, die im Zuge dieser Danksagung unerwähnt blieben, es aber verdienten, genannt zu werden.

Graz, im Mai 2012 Paul Tirk

Contents

CHAPTER 1

Introduction

In the field of atomic absorption spectrometry (AAS) the use of a graphite furnace (GF) for vaporization and atomizing the sample is a long and well established technique. Discovered by Boris V. L'vov in 1956 the GF was also utilized with small amounts of solid samples. The processes of vaporization and atomizing of the analyte both occurred in the same device. With the development of ICP-OES the excitation now took place in the plasma. The commonly employed nebulizer which can only be used with aqueous solutions usually works very inefficient, only a small fraction of the aerosol actually reaches the plasma. Alternatives including hydride generation are solely applicable to a limited number of elements. For these reasons so-called electrothermal-vaporization (ETV) devices were introduced. Like in a GF an electric current is used to heat-up the sample until the evaporation temperature of the desired elements is reached. By choosing the temperature carefully sometimes even matrix separation can be achieved. Many different types and forms were used: carbon cups, graphite tubes, graphite boats, tungsten boats, tungsten coils and other metal filaments. The problem of carbide formation, well known in GF-AAS, also arose in carbon-based ETV devices, especially for refractory materials. By choosing metal filaments – in particular tungsten – several of these difficulties were remedied.

The use of a heated tungsten boat as a vaporization source has been investigated by Nakamura et al. [5]. Good results were achieved using sample solutions combined with time resolved spectrometry. In 2008 Kataoka et al. showed a way to analyze solid iron samples in the tungsten boat furnace (TBF) with ICP-OES [2]. The amount of sample analyzed was similar to the amounts used in solid sampling GF-AAS, i. e . in

the range of mg, resulting in difficulties with homogeneity and potential contamination in sample preparation together with rather high possible errors in weighing. Clearly, it was interesting to investigate if bigger amounts of sample can be vaporized using ETV devices.

To further investigate this subject, it was attempted to design a tungsten boat furnace (TBF) as well as characterizing its possible analytical value in ICP-OES.

This master's thesis is divided into four chapters. Chapter 1 gives a short introduction into the general idea and concepts used in ICP-OES, solid sampling and the TBF. It also includes some additional information about the properties of tungsten and other physical principles which are relevant in some way. The second chapter shows and describes the different parts and their function of the TBF as well as some design considerations. It should include nearly all information important and necessary for constructing and using the furnace. Chapter 3 presents the analytical characterization of the TBF using solid steel samples. Finally the last chapter provides a short summary of the results as well as an outlook towards future work.

1.1. Atomic Absorption/Emission Spectrometry

It is thought that Isaac Newton first discovered the refraction of light when a ray of sunlight accidentally hit a glass prism in his office. But Joannes Marcus Marci of Kronland had already described the origin of a rainbow caused by scattering and refraction of light in water droplets in his book *"Thaumantias. Liber de arcu coelesti deque colorum apparentium natura ortu et causis"* (1648). More observations involving phenomena of sunlight followed. Wollaston discovered dark lines in the sun's spectrum which were named and categorized later by Fraunhofer. Finally Kirchhoff and Bunsen verified the "sodium d-line" by bringing sodium salts into a flame and observing the same line in the resulting emission spectrum. Kirchhoff also declared that matter can emit light of the same wavelength as it absorbs. [10, p. 1-2]

The energy of light having a specific wavelength is given by Planck's law (equation 1.1). According to quantum theory energy can only be absorbed and emitted in

multiples of h, PLANCK's constant[1]. This law is further restricted by the fact that in atoms the electrons can only have certain amounts of energy (which of course must also comply with PLANCK's law), these energies form the basis of the individual spectra for each element.

$$E = h\nu = \frac{hc}{\lambda} \tag{1.1}$$

In all types of spectrometric analysis the amount of light absorbed or emitted by the sample is put in relation to the amount of the corresponding analytes. Ideally one would simply take the intensity of an atomic line – either emission or absorption signal – and relate it to the portion of analyte. In fact atomic lines do not show up as "lines" in the spectrum, there is always a line broadening due to different effects, ranging from DOPPLER broadening up to HEISENBERG's uncertainty principle. Therefore, for quantification, consequently the integral over the whole peak has to be used (equation 1.2). Line broadening effects increase the risk of spectral interference, i. e. signals originating from different elements may overlap to some extend, making it sometimes impossible to obtain the correct integral, even when using a spectrometer with extremely high resolution (< 1 pm). However, these resolutions are not necessary in ICP-OES because of an average emission line full width at half maximum (FWHM) of already around 5 pm.

$$S = \int I(\nu) d\nu \tag{1.2}$$

In atomic spectrometry the analytes ideally should be present as isolated atoms. Then the corresponding atomic absorption/emission lines can be applied for quantification. Normally atomization temperatures are chosen to ensure the necessary equilibrium towards the free atomic state.

The main parts of an optical spectrometer are shown in figures 1.1 and 1.2. It should be noted that the light source is only needed in AAS and can therefore be left out when measuring the emitted radiation of the sample. The monochromator and detector are enclosed in a common housing which is in the case of ICP-OES either evacuated

[1] $h = 6.62606957(29) \cdot 10^{-34}$ Js

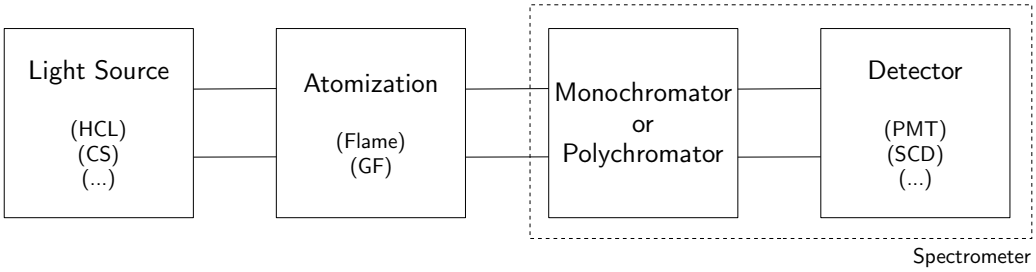

Figure 1.1.: Block diagram of an optical spectrometer used for AAS

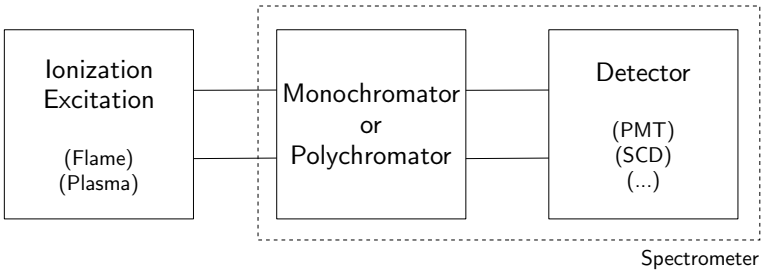

Figure 1.2.: Block diagram of an optical spectrometer used for AES

or filled with an inert gas to avoid absorption of the low ultraviolet radiation (< 200 nm) by O_2 and H_2O which constitutes the most important range of light in atomic spectrometry. In AAS the gas filling is not necessary due to the use of a reference light beam. In addition the spectrometer enclosure is also kept at a constant temperature in order to avoid drifts due to thermal expansion of the optical components. Furthermore, the spectrometer should be widely kept free from vibration. All of these measures ensure a stable environment for detecting the incident light and avoid possible drifting over time thus increasing precision.

1.1.1. Light Source

As absorption is measured in AAS, a light source is needed in the first place. Line sources such as the hollow cathode lamp (HCL) are among the earliest radiation sources in AAS and nevertheless still widely used nowadays. A HCL consists of a cathode which is made of the element whose atomic lines should be emitted and an anode, both situated in a glass cylinder filled with a noble gas. By applying a high voltage between

the two electrodes the gas gets ionized and the electrons become accelerated towards the hollow cathode. When striking the surface atoms get sputtered off which in turn collide with other electrons and reach their excited states. Due to the finite lifetime of the excited states the atoms will return to their ground state while emitting light. This produces the desired atomic spectrum of a specific element as well as a few additional lines resulting from excitation of the noble gas filling.

In contrast to HCLs a continuum radiation source emits light of many wavelengths at the same time thus forming a "continuum"[2] of light. In principle it could be a simple lightbulb but emission is not strong enough in the ultraviolet part of the spectrum. An extensively used example is the high pressure xenon short arc lamp. Having a wavelength range from 190 up to 900 nm makes it a useful source of light for AAS.

1.1.2. Atomizer

The atomizers purpose is transforming the analytes which are bound in molecules into their free atomic state. This ensures the known atomic absorption/emission lines can be monitored for acquiring the signal representing the desired quantity. In an inductively-coupled plasma (ICP) additionally the excitation of electrons occurs leading to the emission spectrum used for evaluation. Over time different types of atomizers evolved, some of which are shortly described below.

Flame Atomizer

The probably simplest method to do spectroscopy is by using a flame as an atomizer. This was done by Kirchhoff and Bunsen to prove the sodium spectrum. The coloring of a flame by burning different metal salts – preferably alkali or alkaline earth metal salts – has most likely been observed by the reader himself during his life. It was clearly the first step to further investigate this phenomenon by improving and systematizing the procedure. One step was to let the flame burn through a slit so it provides a defined optical path length which is equivalent to the path length d used in Lambert-Beer's law (equation 1.3), one of the fundamentals of AAS. But as the

[2]Since we recall Planck's law (equation 1.1) a real continuum light source can not exist.

flame is also being used to excite the atoms either the emission produced by the analyte or the absorption can be measured by the spectrometer. Figure 1.4 shows a picture of a flame atomizer while in use.

$$E = \log\left(\frac{I_0}{I}\right) = \epsilon \cdot c \cdot d \tag{1.3}$$

Graphite Furnace Atomizer

A graphite furnace (GF) was first used as an atomizer by Boris V. L'vov in 1956. Strictly speaking he cannot be named as the inventor but rather utilized an electrically powered device for the first time for AAS. During his investigation he realized that in order to avoid loss of analyte through diffusion, the sample has to be heated very quickly. Later he refined this statement by proving the direct relation between integrated absorption and sample mass. In the age of modern computing the former can easily be evaluated.

The GF is essentially a graphite tube containing the sample which is heated up to around 2500 K by applying an electric current. During measurement the excitation light is shining through the tube. Both transversally and longitudinally heated variants exist, sometimes additionally equipped with an electromagnet to make use of the Zeeman effect.

Inductively Coupled Plasma

Although technically not exactly regarded as an atomizer the ICP nowadays belongs to the most widely used atomization/ionization sources in atomic spectrometry. A plasma is known as a distinct state of aggregation wherein the electrons become separated from the nuclei. In an ICP the energy needed for achieving such a state is introduced by applying an electromagnetic alternating field produced by a radiofrequency (RF) generator to a coil which is wound around a concentric set of quartz tubes, termed "plasma torch". A small pipe in the middle – the injector – serves as the sample inlet (refer to figure 1.3). The current in the coil induces an corresponding current in the plasma gas which causes a separation of charge, i. e. the negatively charged electrons

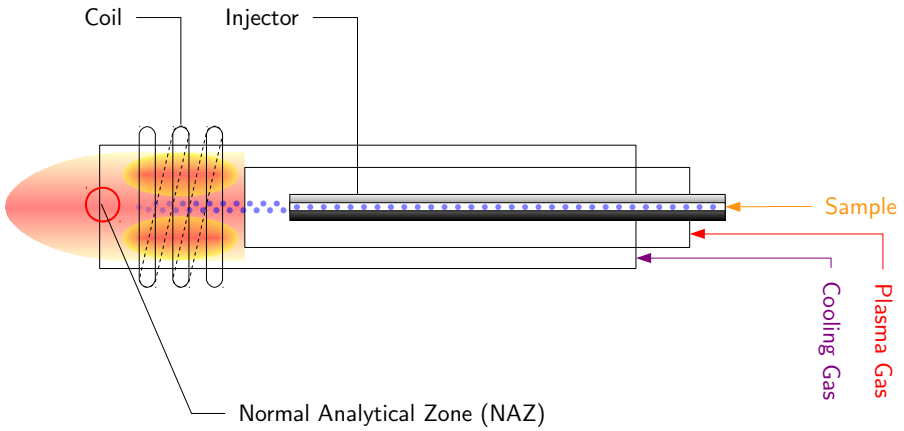

Figure 1.3.: Drawing of a plasma torch

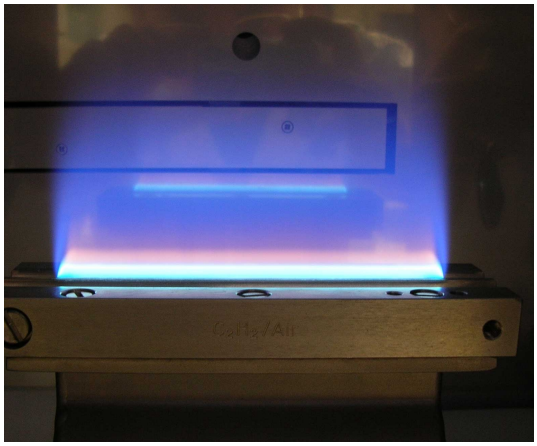

Figure 1.4.: Photography of a flame atomizer

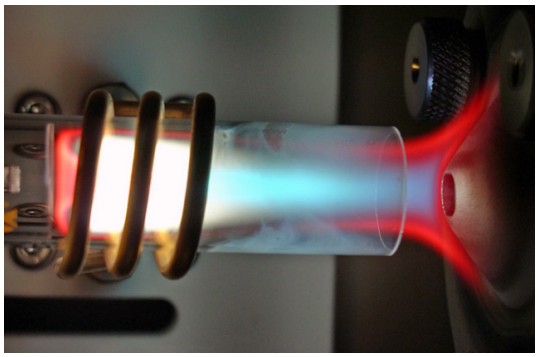

Source: http://www.aktuelle-wochenschau.de/2009/images/w12/abb3.jpg (25.03.2012)

Figure 1.5.: Photography of an ICP

are moved in the other direction than their corresponding nuclei. If the induced energy is high enough they get separated and form the plasma.

The plasma itself is located toroidally in the torch, having temperatures of around 10000 K. The sample aerosol or vapor (in case of solid sampling) is brought into the centre of the plasma toroid through the injector. The temperature here is slightly lower, about 8000 K but still sufficiently hot that almost all existing molecules are broken into atoms, keeping the method virtually free from influences of chemical bonding.

1.1.3. Monochromator/Polychromator

The monochromator serves by dividing the incoming light into a spectrum of individual wavelengths which can afterwards be detected and quantified by the detector. Depending on the detector it is sometimes needed to scan over all wavelengths of interest implying a longer time necessary to complete one measurement. Some detectors are capable of registering a wider range simultaneously thus shortening the time of the analysis. It is even possible to acquire time-resolved data, while time resolution strongly depends on the time used for completing one set of data. The result of such a measurement are peak profiles showing the temporal progress of the analyte signal which is especially useful while optimizing atomization and vaporization temperatures, for example in a GF or the TBF.

If the detector is able to evaluate multiple wavelengths at the same time, or even the full spectrum, we speak of a polychromator. This ability poses a huge gain in time as the "scanning" action needed when using a monochromator becomes obsolete. As a downside a high spectral resolution requires many detector elements and a more complex construction, making the device more expensive.

1.1.4. Detector

The aim of the measurement is a value representing the desired quantity of analyte. In spectrometry this is done by evaluating the intensity of light. The detector therefore has to convert the incident photons into a signal which can then be further processed by the connected electronics and stored consecutively. The most common types of detectors and their operating principles are explained briefly in this section.

Photomultiplier Tube

The photomultiplier tube (PMT) or secondary electron multiplier originated long before the invention of semiconductor devices and has not vanished since because of its very high sensitivity, under certain circumstances being able to register even a single incident photon but at the cost of a worse signal-to-noise ratio (SNR). Basically it consists of a

photosensitive electrode which emits an electron when hit by a photon. These so-called secondary electrons are then multiplied by a cascade of dynodes connected to different electric potentials in the range of a few hundred volts. The multiplication occurs by accelerating the electrons from one dynode to another, each releasing more electrons. At the end of the cascade the resulting current can be measured. The big advantage compared to semiconductor devices (section 1.1.4) is the ability to vary the gain while leaving the integration time of the detector fixed. This can be done simply by changing the voltage of the dynodes.

Semiconductor Detector

With the invention of semiconductor diodes they were gradually being used as photodetectors. Basic principle is the inner photo effect of a pn-junction. Like in PMTs a photon can excite an electron causing charge separation which in turn produces a photocurrent. The big advantage is the possibility to arrange several of this diodes in lines or arrays of detector spots, obtaining spatial resolution and enabling the measurement of multiple wavelengths at the same time. The major downsides of semiconductor detectors are the lesser sensitivity and the greater detector noise, bringing up the need for constant sub-zero cooling. Also, signal intensities depend on integration time.

1.2. Solid Sampling

Traditionally – apart from a few exceptions – spectrometric methods use liquid solutions for calibration and as samples. This produces some further implications which are to be described shortly together with potential advantages of solid sampling as well as problems arising.

Every step taken to transform a sample into a suitable measurable form, i. e. a liquid solution, bears the risk of contamination and introduces to some extend loss of analyte as well as additional errors hence deteriorating the result and recovery rate of the analysis. Required dilution decreases the already small analyte content even more and combined with poor sample introduction efficiency sensitivity becomes reduced significantly. For example, in ICP-OES the commonly employed pneumatic nebulizers

have an efficiency of around 1-5 %. Besides, they behave problematically when used with viscous solutions, samples of high salt content or when only small sample volumes are available.

Therefore direct solid sampling inherently possesses higher sensitivity as no further dilution occurs and the analyte is introduced into the analyzing system more efficiently, lowering the limits of detection (LODs) substantially. Moreover, sample preparation is essentially reduced to homogenizing and weighing, thus saving time and avoiding rather corrosive and potentially hazardous reagents. This also results in economic and environmental benefits. Without the need of sample digestion and the accompanying dilution the risk of contamination as well as the risk of analyte loss is greatly reduced, although not completely eliminated as sample processing can still cause cross-contamination. So far all the available solid sampling techniques use rather small sample amounts, which on the one hand makes it easy to volatilize all of the analyte but on the other hand requires high precision in weighing to avoid errors, while sample homogeneity becomes one of the most demanding aspects.

Often in industrial processes monitoring of trace elements by liquid analysis is only accessible in the final product, as the time-consuming sample dissolution procedure is not applicable to each production step. A suitable solid sampling technique could remedy this limitation.

Calibration as well as data evaluation also have to be handled differently as all solid sampling methods produce rather complex time-resolved signals as opposed to "steady-state" measurements employed in conventional solution-based analysis [4].

In ETV based solid sampling the boiling temperature of the analytes is a crucial factor and in certain cases it may be necessary to use additional chemical modifiers which alter the vaporization characteristic in a way that evaporation is achieved. Such technique for example can be based on the forming of an eutectic mixture, which possesses a lower melting point [2]. When using liquid solutions other possibilities include hydride technique or volatilization by chelation of metals. The potential separation of the matrix elements from the analytes is of particularly high interest when it comes to avoiding spectral interferences. A lower vaporization temperature also can contribute to an increased lifetime of the ETV device.

Finally it should be emphasized that in the case of solution based analysis the desired number of replicates is taken from the same sample (solution), averaging over fluctuations in the measurement process, while in solid sampling one would have to use new material for every "shot", i. e. measuring "true" replicates.

1.3. Tungsten

Looking at the properties of tungsten one can easily understand why it is the element of choice for ETV. First of all its melting point is around 3400 degrees celsius, the highest among all metals and also far beyond the ones of elements typically analyzed. Furthermore it appears to be the element with the lowest vapor pressure even at very high temperatures [1]. A low thermal expansion coefficient, the high chemical inertness and its extraordinary wettability towards molten solids, which causes the distribution of the sample over the total surface, resulting in better evaporation of the analytes, contribute to its great suitability as an ETV device. The problem of carbide formation – inherent to graphite based ETV devices – is completely eliminated. Moreover a smaller thermal gradient and a relatively long lifetime of tubes and boats add to the advantages of tungsten over graphite. Despite its outstanding properties tungsten is still available at reasonable prices – probably due to its broad use as lighting filaments – and it can be obtained directly in various forms like foils, sheets, powder, strips, boats and may others.

1.3.1. General Properties and Appearance

Tungsten is regarded a metallic transition element having 74 protons and 84 to 116 neutrons. Considered the 56^{th} most abundant element in the earth's crust and number 18 among the metals it can be found in rocks where it is bound in its oxidized form as the hexavalent ion W^{6+} [3, pp. 1-2, 65]. Like all metals its appearance is that of a shiny grayish steel-like material (see figure 1.6). In its pure form it is barely ductile (depending on its thickness) but rather brittle and should therefore handled carefully as it cracks very easily.

Heinrich Pniok (www.pse-mendelejew.de), License: CC-BY-NC-ND

Figure 1.6.: Tungsten rods with crystals and 1 cm^3 tungsten cube

1.3.2. Chemical Properties

Although considered rather inert a wide range of tungsten compounds exist. Of particular interest is the formation of a number of oxides posing the risk of deterioration and damage to the metal especially at higher temperatures. Experiments must therefore be carried out under exclusion of oxygen and water either in vacuum or under inert gas atmosphere. Apart from that, surface reactions occur with nearly all metals. This sometimes bears high technological interest but as a metal filament in ETV applications it is rather undesired (see also section 4.2). Figure 1.7 summarizes the reactivity of tungsten.

1.3.3. Vapor Pressure

In order to be able to vaporize an element by heating it on a tungsten strip its vapor pressure obviously should be higher than the one of tungsten. Figures 1.8 and 1.9 show the vapor pressure curves of tungsten as well as of some other elements of interest. It is easily seen that one of the outstanding properties of tungsten is its very low vapor pressure, a highly desirable property of ETV devices. Nevertheless at high

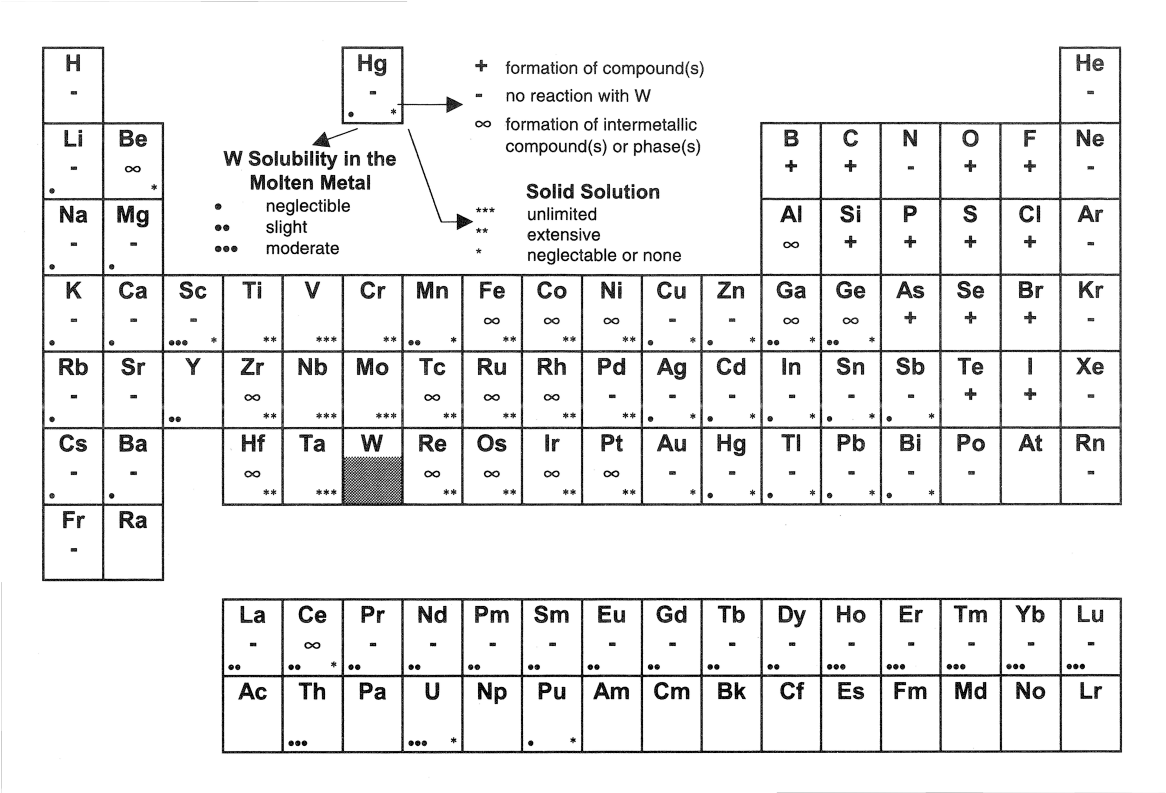

Figure 1.7.: Periodic table of elements indicating reactions with tungsten [3, p. 44]

temperatures a significant amount of tungsten is evaporated. This tungsten vapor can cause spectral interferences in AAS and ICP-OES due to its high number of electrons and therefore many possible transition energies (refer to figure 3.1).

1.3.4. Heat Capacity

In order to heat a substance one has to provide energy. The amount of energy needed for increasing the temperature of a specific material is given by its heat capacity, normally expressed in $\mathrm{J\,mol^{-1}\,K^{-1}}$. Generally, the heat capacity is not constant over temperature as shown in figure 1.10. To get the energy necessary for bringing one mole of a certain matter from its current temperature T_1 to a new one T_2 the curve needs to be integrated.

$$Q = \int_{T_1}^{T_2} C_p(T)\ \mathrm{d}T \tag{1.4}$$

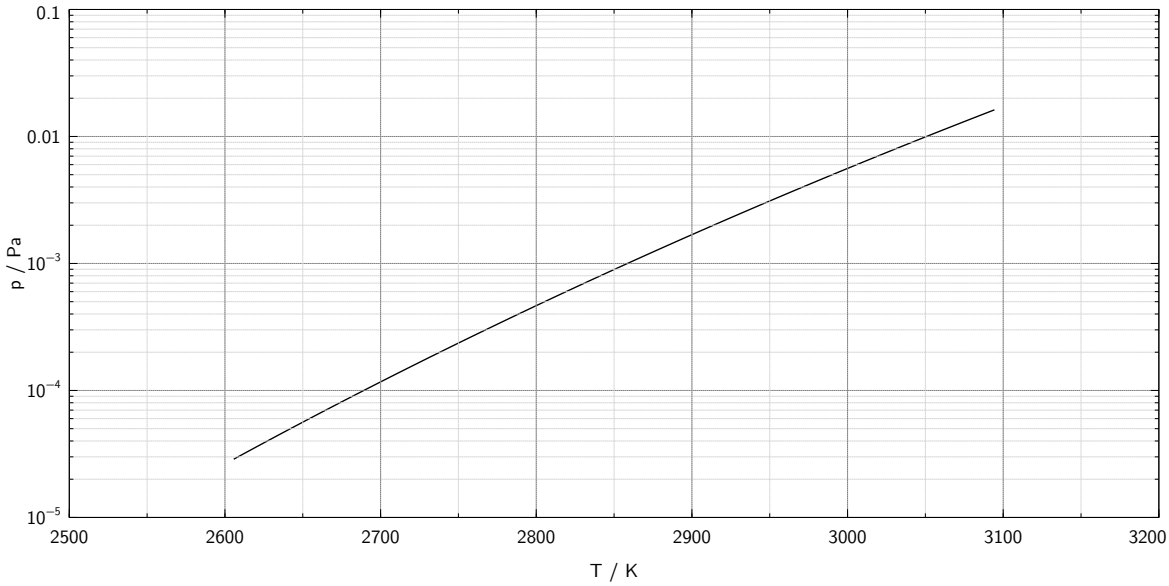

Figure 1.8.: Vapor pressure of tungsten [8]

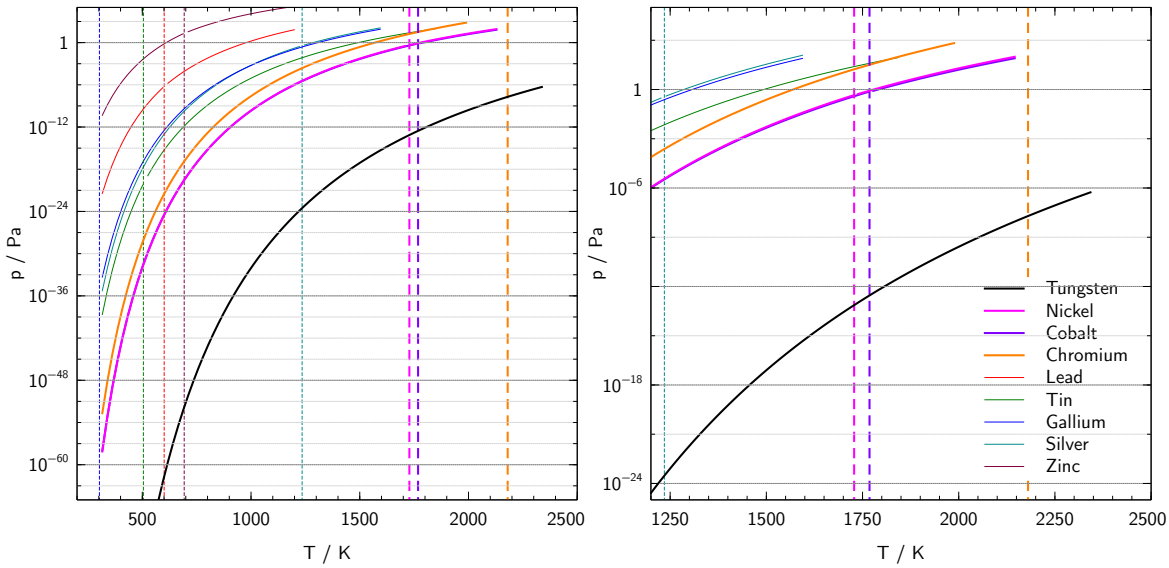

Figure 1.9.: Vapor pressures [1, p. **4**-124f.]

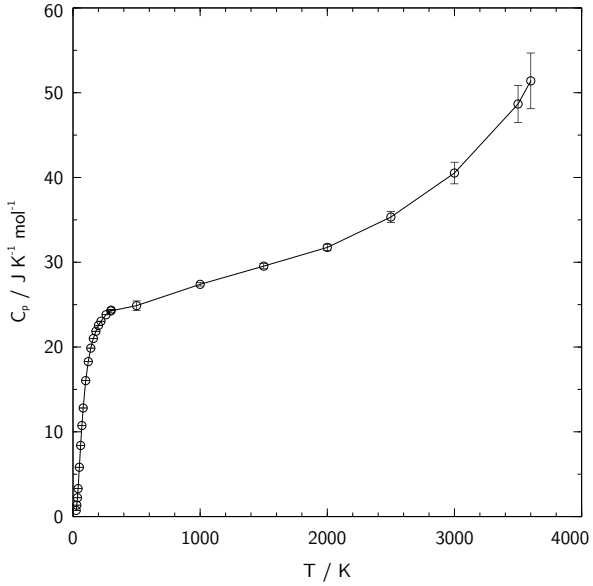

Figure 1.10.: Heat capacity of tungsten [3, p. 32]

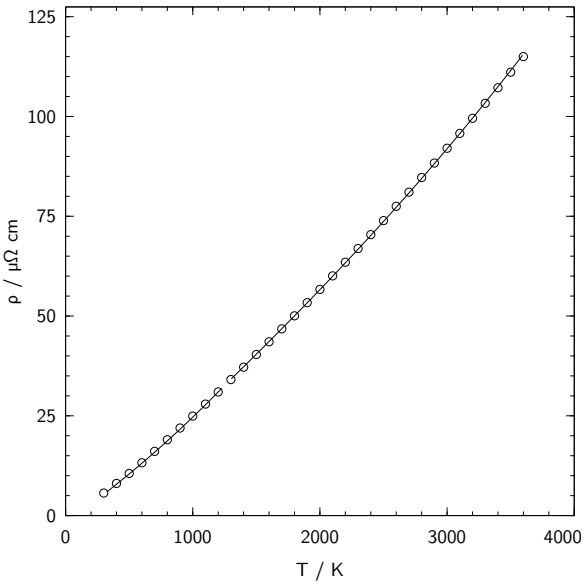

Figure 1.11.: Electrical resistance of tungsten [3, pp. 34-35]

In a metal strip furnace the energy is brought into the system by applying an electric current which due to the intrinsic resistance of the filament causes the desired increase in temperature. As this process occurs in a finite amount of time, the maximum rate of heating is set by the electrical power the power supply is able to deliver.

$$P = \frac{Q}{t} = U \cdot I \tag{1.5}$$

The voltage drop over an ohmic load is always proportional to the current flowing through it, while the proportionality factor is the resistance (see section 1.3.5).

1.3.5. Electrical Resistance

As a metal the electrical resistance of tungsten at room temperature (25 °C) is in the range of a few $\mu\Omega \cdot \mathrm{cm}$. As shown in figure 1.11 it increases with temperature, thus having a positive temperature coefficient. As a consequence – according to Ohm's law – the rising voltage drop across the metal causes higher power dissipation leading to an increase in temperature itself. Still, even at high temperatures tungsten behaves rather as a conductor and there is no need of a high voltage to drive a large electric

current through the metal. Hence it is desirable to provide large currents as they are needed for heating up the tungsten strip rapidly. The next chapter will further discuss the steps taken to achieve as much current as possible.

CHAPTER 2

Design and Construction

This chapter describes the process of designing and constructing all the parts necessary for the TBF. It includes the most important specifications and decisions which were made during the development. The apparatus essentially consists of two parts: the actual furnace and its variable and programmable power supply.

2.1. Tungsten Boat Furnace

The furnaces main purpose is to heat up the sample, vaporize the analytes and transport these vapors into the analyzing instrument, e. g. the ICP-OES. This is done by heating a small strip of tungsten to a sufficiently high temperature. The metal strip should be in tight contact with the sample. Conveniently so-called tungsten "boats" – which are widely used in metal vaporization and deposition – can be employed for this purpose.

The tungsten strip is heated by a rather large electric current, thus it has to be fixed tightly between two electrodes for low contact resistance. The generated vapors need to be flushed out of the furnace into the atomizing and analyzing device. This is simply done by a continuous gas flow entering the cavity from below the tungsten boat through a hole. On top a modified glas frit (filter was removed) was used to seal off the surroundings and provide the vapor outlet at the top. The whole system is flushed by an inert gas such as argon because tungsten oxides are formed rapidly in the presence of oxygen or water vapor eventually making the metal strip brittle. The subsequent

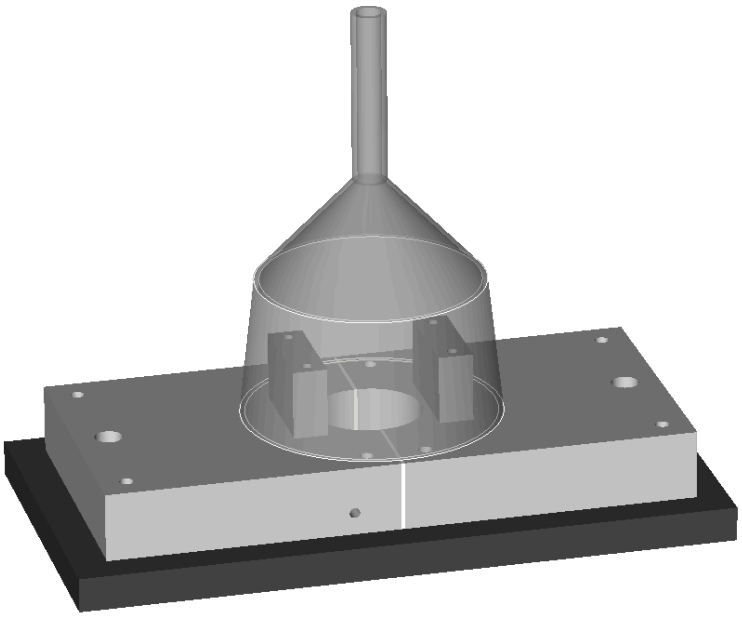

Figure 2.1.: Rendered model of the tungsten boat furnace

evaporation of the oxides can even disintegrate the boat severely. By situating the gas inlet tangentially on the cavity floor it was hoped to generate a turbulent gas flow which should flush most of the vapors out of the furnace efficiently. Figure 2.1 shows a model of the assembly of the TBF.

The two electrode blocks were made of aluminium. On the bottom side two commercial CPU water-coolers were mounted. A small strip of polytetrafluorethylene (PTFE) provides isolation between the electrodes. The whole assembly is mounted on top of a polyvinylchloride (PVC) board. To avoid contact resistance due to the connection to the power supply (see section 2.2) the output transformer's secondary winding was connected directly to the electrodes. This also required the transformer itself to be placed behind the tungsten boat. Figure 2.2 shows the actual prototype[1].

Previous experiments have shown that adding a small amount of hydrogen to the argon stream can further prevent oxidation [7]. This was done using a mass flow controller (100 sccm, MassFLO™, MKS, Germany). Furthermore loading the sample onto the tungsten boat requires removing the glass frit and thereby introducing air into the furnace. This raised the need to flush the TBF again before firing. Figure 2.3

[1]In the photographs the TBF does not contain the transformer as it was removed again for the use of an other power supply (refer to section 2.4).

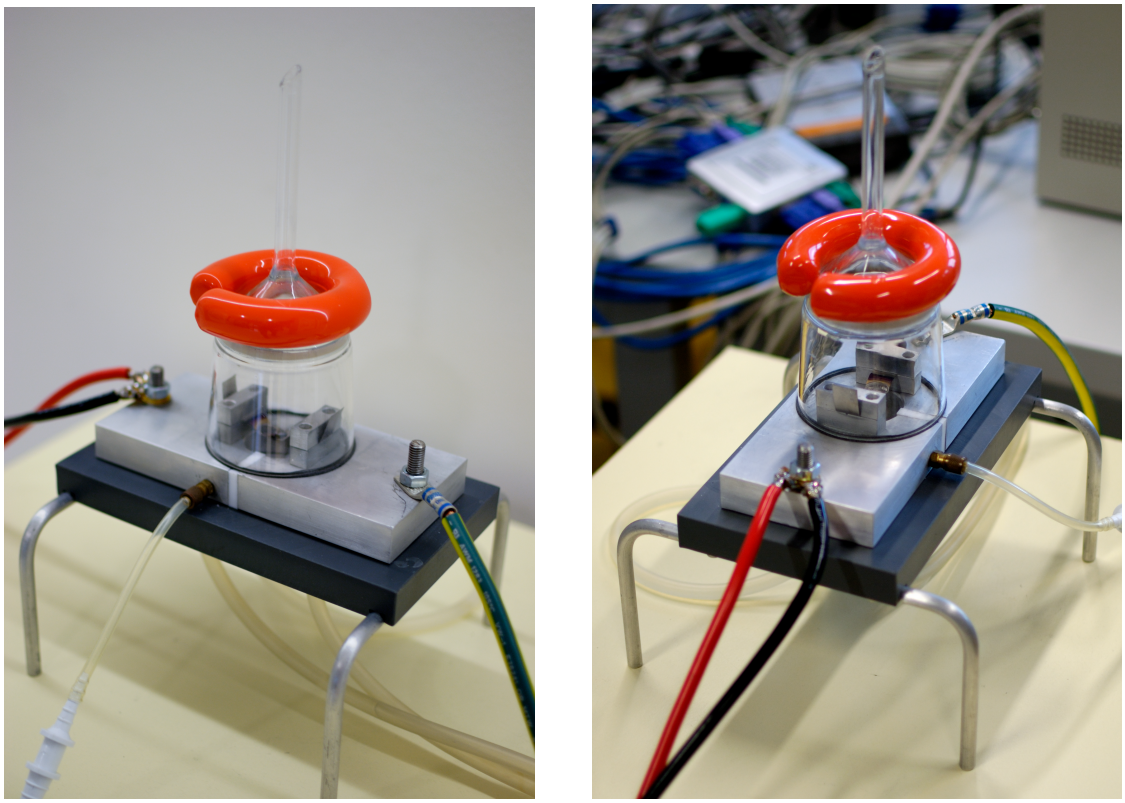

Figure 2.2.: Tungsten boat furnace prototype

Table 2.1.: Valve settings sequence

Status	Action	Valve Status		
		V_1	V_2	V_3
Sample loading	open V_1, V_2 to "ventilation", close V_3, remove frit, load sample, reattach frit	open	ventilation	closed
Preflushing	V_3 to "Ar"	open	ventilation	argon
Flushing	V_3 to "Ar/H_2 mixture", V_2 to "ICP-OES", close V_1	closed	ICP-OES	Ar/H_2 mixture
Measurement	–	closed	ICP-OES	Ar/H_2 mixture

pictures the gas connections and valves used for bypassing the furnace during sample loading/change as well as the power and cooling water supplies. In addition the proper operating sequence is described in table 2.1.

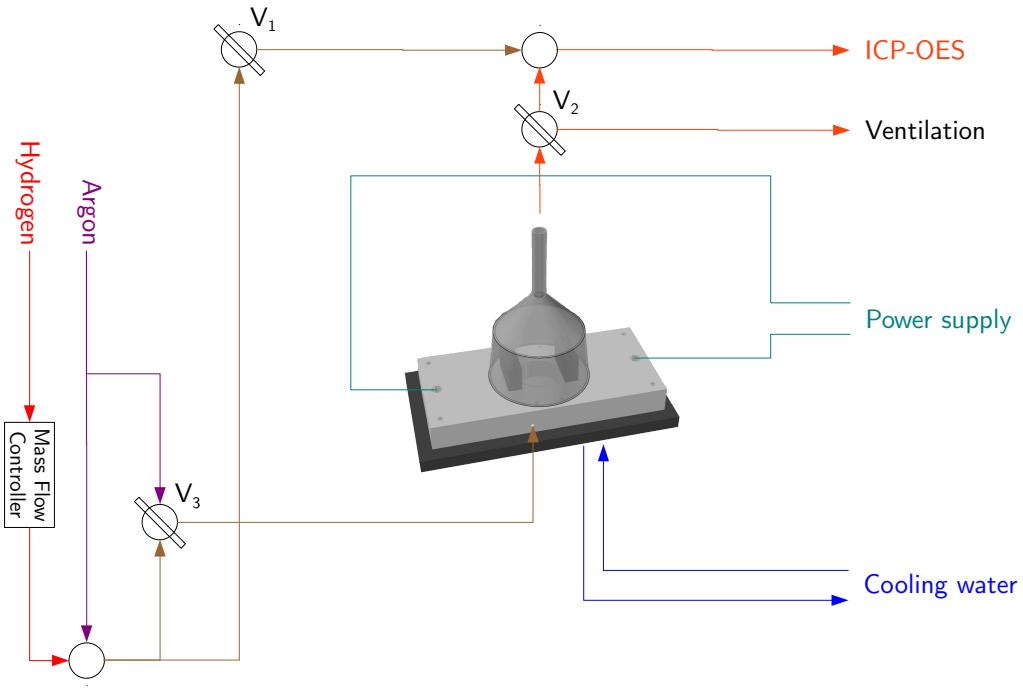

Figure 2.3.: Connection diagram

2.2. Power Supply

During the search for information regarding a suitable power supply we had to recognize the fact that devices able to deliver currents in the range of a few hundred amperes are not affordable by our budget. Hence it was decided to accept the challenge and build one ourselves. Considering efficiency and size in this power range the device of choice was of course a switching power supply (SPS). The following sections describe the general building blocks of the SPS as well as the used circuits when appropriate. Also a short introduction regarding the functional principles of a SPS is given.

2.2.1. Switching Power Supplies

Conventional power supplies consisting of a mains transformer, a rectifier and a linear voltage regulator suffer from relatively large losses when it comes to higher power demands. Apart from being terribly inefficient it grows more and more difficult to

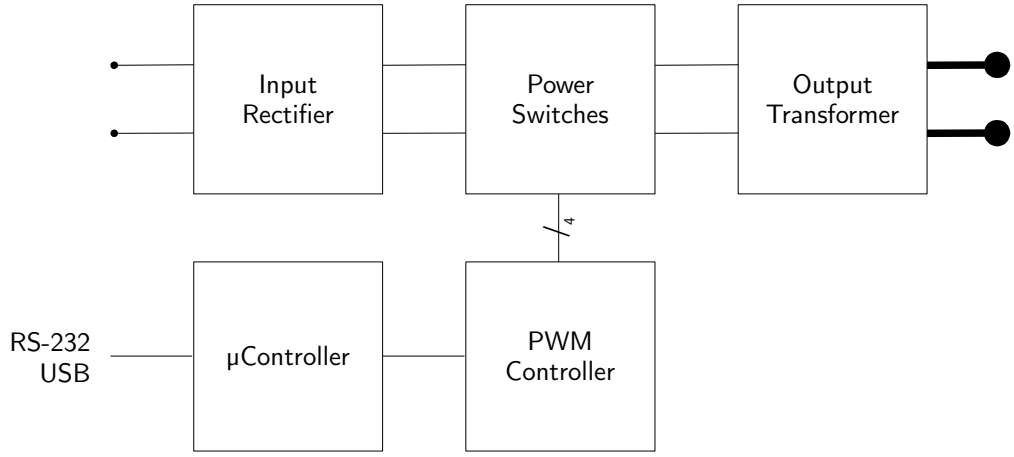

Figure 2.4.: General composition of a switching power supply

get rid of the produced heat. For these reasons so-called "switching power supplies" (SPS) are used nowadays. Simply spoken, a SPS – as the name implies – generates the desired output power by switching on the main voltage (most often the power line voltage) during a specific amount of time and turning it off again. When the average of a whole switching period is taken the power transferred to the output is proportional to the "on" time. By varying the "on" fraction of the switching period one can set the output power as needed.

Figure 2.4 shows the building blocks of a SPS. The mains current is being rectified and then fed to the power switch. The switched current could then be smoothed and used directly or – if isolation and/or voltage scaling is desired – applied to the primary winding of a transformer. The transformers secondary is then normally smoothed and rectified again providing the desired direct current (DC) voltage.

2.2.2. Building Blocks

The specifications of the needed power supply are chosen according to the properties of the used metal strip. Electrical specifications are available from manufacturers of tungsten boats utilized widely in metal vapor deposition systems, providing approximate values of voltage and current for heating the boat. Among the various topologies of SPSs the full bridge was chosen because of its ability to handle high power and voltage

Table 2.2.: SPS specifications

Property	Value	Unit
Input voltage	230	V
Input current	max. 16	A
Output current	250	A

stresses (see section 2.2.4). Moreover, it is not necessary to supply direct current for heating a GF or a TBF. This simplifies the design by eliminating the need for the output rectifier, which would have to be capable of delivering 100-200 A. As a consequence the secondary winding of the transformer is directly connected to the electrodes.

2.2.3. Input Section

The first part of the developed power supply is the input section whose purpose is to rectify the input voltage, i. e. converting the alternating current (AC) of the mains line into a DC. It also includes a power line filter to avoid feeding back the high frequency switching noise from the power section (section 2.2.4) into the building's power system. After rectification the current is smoothed by capacitors (four 1500 µF capacitors), able to withstand a voltage of 350 V each. The four capacitors are connected in parallel thus providing a total capacity of 6000 µF and a voltage rating of 350 V. As a safety measure an additional bleeding resistor discharges the capacitors after the main voltage is removed. The rectified and smoothed DC voltage is then fed to the power switches. In order to limit the large inrush current into the capacitors at turn on of the device, a resistor was incorporated just before the capacitors. It is shunted after a few seconds by a relay. The time delay is controlled by the microcontroller (refer to section 2.2.6).

2.2.4. Power Section

The power section consists of four metal oxide semiconductor field effect transistors (MOSFETs) which act as the power switches. They are arranged in a so-called full bridge topology (see figure 2.5). The MOSFETs are switched in such manner that

a current is flowing through the main transformer's primary winding alternately in either direction. This means either transistors A and D or B and C should be on at the same time. In order to turn on a MOSFET the gate has to be charged sufficiently which is done by a special driver IC (IR2110). The upper two field effect transistors (FETs) (A and C) need special attention because their gate circuits are floating about 300 Vabove ground potential. The IR2110 overcomes this problem by shifting the gate voltage accordingly thus providing the necessary high-side driver circuitry. Depending on the switching state of the FETs a current flows through the main transformer's primary. The resulting magnetic flux change then induces a current in the secondary winding which is indirectly proportional to the turns ratio of the main transformer.

Each MOSFET is protected by two diodes with very low reverse recovery time, allowing current through the transistor only in one direction. After each switching cycle a reverse voltage spike from the transformer occurs which is drained by the four bypass diodes. In addition a suppressor diode (not shown in the schematic) protects the MOSFETs from possible over voltage spikes between their drain and source pins. The gate circuit consists of a zener diode, limiting the gate voltage to 16 volts and two different series resistors, one bypassed by a diode, allowing distinct switching speeds for turning the FET on or off. This is to avoid turning on the high side FET together with the low side one in the same half of the full bridge as a very high voltage rise at the low side FET could cause charging of the gate through the parasitic miller capacitance and thus leading to significant cross-conduction and eventual destruction of the MOSFETs. This phenomenon is also known as "shoot-through".

It also turned out that the layout of the printed circuit board (PCB) is a very crucial part when it comes to operating frequencies in the range of a several kHz. Especially when dealing with high currents the parasitic inductance of the PCB traces can cause large voltage spikes, eventually causing problems in the MOSFETs (refer to the above described "shoot-through"). Therefore trace lengths should be reduced to a minimum. Another important issue involves current return paths. With increasing signal frequency the resulting current loop of a signal tries to use the same route for its signal and return paths. As a consequence potential return paths (for example in copper planes) should not be interrupted by other traces. Because of the rather big gate currents it is also beneficial to make use of wide tracks.

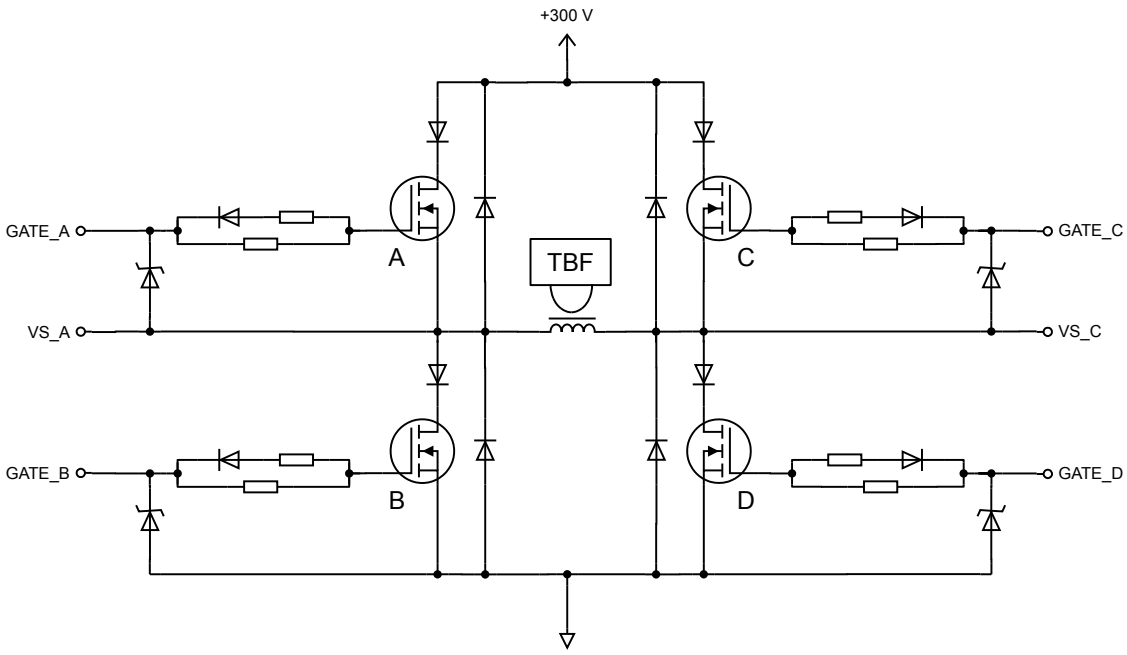

Figure 2.5.: Power section circuit

Moreover, it became clear that many of the remaining voltage spikes can be damped by good bypassing of the power supply. This involved employing foil capacitors (around 20 µF) mounted as close as possible to the supply rails of the power switches. It seemed that – as mentioned before – every cable should be as short as possible as its inherent inductance diminishes the desired effect of the capacitors.

2.2.5. PWM Controller

As mentioned in section 2.2.4 the power MOSFETs drive circuitry needs to be activated at the right times. This is done by the pulse width modulation (PWM) controller. In this design a UCC3895 controller chip of Texas Instruments was used. The UCC3895 is able to provide pulses for driving full bridge topologies by activating its four outputs accordingly. The outputs are then fed into the IC2110 half-bridge drivers which provide enough current for charging and discharging the MOSFETs' gate. Each driver IC consists of a high-side driving circuit, which is needed because the source potential of the high-side FETs A and C is floating between nearly ground and positive supply

voltage, and a driver for the low-side transistors (B and D). The charge loading the high-side MOSFET's gate is intermittently stored by the so-called bootstrap capacitor. For turning on the transistor this charge is then shifted up to the power supply voltage by a level-shifting circuit integrated in the IC2110.

The pulse width modulation is achieved by introducing a phase shift between the switching of the two output pairs A/B and C/D. The controller also features current sensing and dead time modulation. During the dead time none of the power MOSFETs is conducting. It is necessary to ensure that any cross-conduction is avoided. In certain designs (e. g. zero voltage switching) the efficiency of the power supply can be improved by adapting the dead time to the current flowing through the bridge, although this feature was left unused. Figure 2.6 shows the typical gate drive waveforms of the high-side switches. The upper part was recorded with a phase shift of practically zero, while in the lower part the phase shift producing the desired duty cycle can be seen just before the end of the rectangular pulse. When the low-side FET switches, some ringing occurs and can also be monitored in the high-side FET's gate waveform. During the fraction of time between the ringing and the end of the pulse one leg of the full bridge is on, allowing current to flow through the load – in this case: the main transformer.

The current sense function limits the current flowing through the bridge and the primary winding by cutting off the pulse when the voltage on the current-sense-pin of the IC rises above a fixed threshold. If the voltage continues rising above a second threshold the controller puts itself into soft-start mode. The outputs are shut down until the voltage on the current-sense-pin has fallen again. The voltage for the current sensing is induced in a second current transformer which was constructed by drilling a hole through an inductor. The cable to the primary winding of the main transformer is routed through the hole and hence serves as a single turn primary of the sensing transformer. To suppress eventual spikes in the current-sense signal it proved useful to employ a simple first-order low-pass filter.

The actual width of the current pulse – and therefore the current through the transformer – is controlled by applying a voltage to the non-inverting input of the error amplifier, an operational amplifier incorporated into the PWM controller. This voltage can either be manually set by a potentiometer or be generated by the microcontroller (see section 2.2.6). As the ouput power is proportional to the pulse width the tungsten boat can be

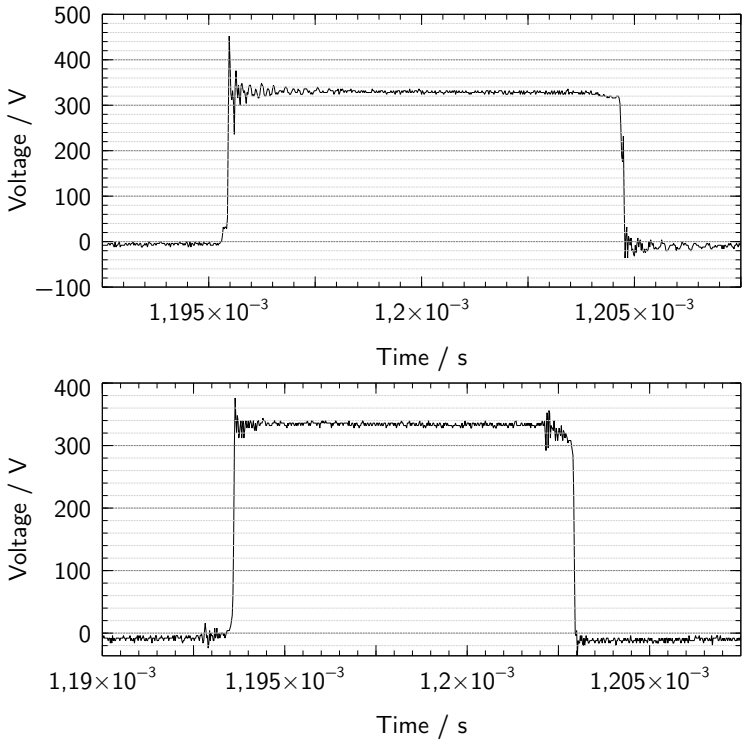

Figure 2.6.: Gate waveforms

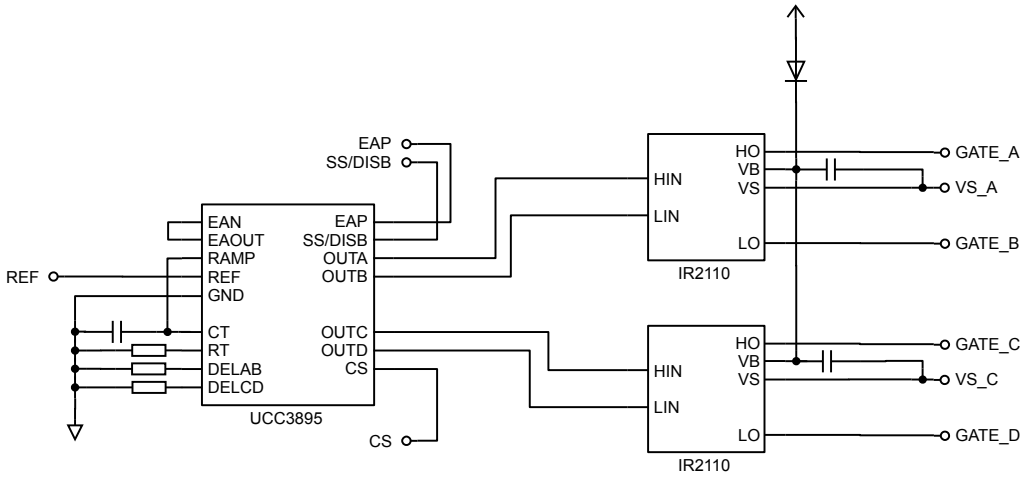

Figure 2.7.: PWM controller circuit

heated according to the desired temperature program by setting the error amplifier's voltage correspondingly.

2.2.6. Microcontroller

For convenient control of the furnace's operation a microcontroller-based solution was used. The interface is provided by a set of commands sent through a standard USB connection emulating a RS-232 serial console. The microcontroller processes the received command and sets all the parameters of the power supply accordingly. It is also able to control the operation of other distinct parts in the setup. For increased protection of the personal computer (PC) side the RS-232 connection was fully isolated from the USB part by optocouplers.

Due to high availability and previous experience an Atmel™ ATmega32™ controller was the chosen. It provides a high number of configurable IO-pins as well as eight analog-digital converters (ADCs), a universal asynchronous receiver/transmitter (UART) and other peripherals easily programmable in C. Part of the microcontroller's memory was used for a boot-loader, which allows updating of the firmware conveniently over the USB port. The device was extended by a digital-analog converter (DAC) from Texas Instruments (TLC5620) which provides four additional analogue outputs and is programmable like a serial shift register by using only three IO-pins of the controller. One of its outputs is directly connected to the error amplifier of the PWM controller (see section 2.2.5), setting the duty cycle in proportion to the generated voltage. The remaining three DAC ports could be used as additional control voltages for providing other features like setting different gas mixtures using mass flow controllers. Another add-on was a ULN2003 IC which provides seven darlington-transistor drivers, each capable of delivering 500 mA, enough for switching relays, driving small motors or other peripheral devices. The remaining pins of the microcontroller stay available as general I/O ports.

The internal ADCs can be used to connect temperature probes allowing constant monitoring of the heat condition in the power section and the electrodes of the TBF. As the tungsten filament reaches temperatures up to 3000 K a contact-less measurement of the temperature is needed to determine the temperature of the sample evaporation site itself. These instruments, known as pyrometers, work by observing the infrared (and

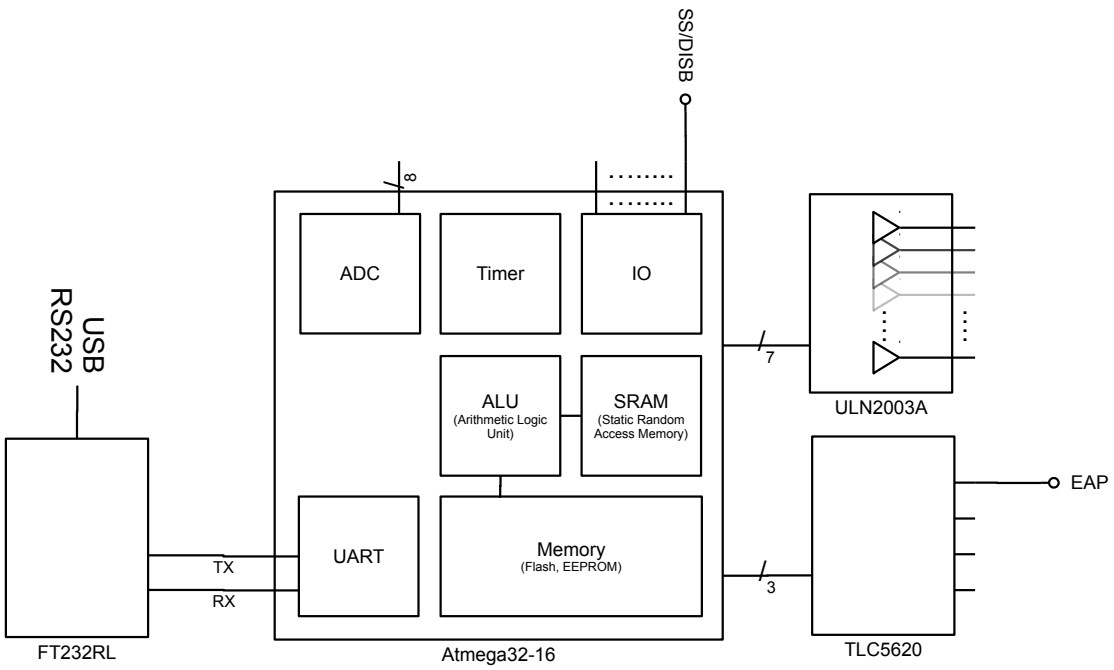

Figure 2.8.: Microcontroller circuit

visible) radiation of an object – in this case the tungsten metal strip – and together with the appropriate emissivity the temperature can be calculated. Unfortunately due to the high costs it was not possible to apply such temperature monitoring to the measurements.

Table 2.4 summarizes the commands of the controller. Each command is sent using the RS-232 interface. The controller responds according to its processing state. While busy no command can be entered. The table is divided into three parts which correspond to the three operating modes of the controller: discontinuous, continuous and program mode. Discontinuous mode allows to heat the tungsten boat to a fixed temperature for a also fixed time. It could be described as "firing" a single "shot". Obviously the TBF would have to be temperature calibrated first, as the microcontroller can only regulate the output power of the power supply. Without a pyrometer this was not achievable so far but nevertheless the commands were implemented for future use. In continuous mode the output power is activated and can then be varied by sending the adequate commands. The last mode – program mode – allows the user to set the desired heating cycle at once, being able to "fire" the same sequence multiple times by running the program. The sequence itself is constructed by a chain of different

Table 2.3.: Furnace program instructions

Action	Description
`;Ttime`	Wait for `time` seconds.
`;Rtemp time`	Change to `temp` using a linear ramp of `time` seconds.
`;Ddutycycle time`	Change to raw duty cycle value `dutycycle` by applying a linear ramp of `time` seconds.
`;Vdac value time`	Change to DAC output value `value` of DAC number `dac` within the time `time`.
`;O1`	Turn output on.
`;O0`	Turn output off.

actions and can be saved to or read from the microcontroller's electrically erasable programmable read-only memory (EEPROM) as a string. Table 2.3 shows the available elements, while an example of of a possible furnace program is listed below:

```
;D0 0;O1;T2.0;R300 4.0;T4.0;R500 5.0;T4.0;R2000 3.2;T2.0;D0 0;O0
```

Additionally there are some system commands which control basic functions like switching of the main relay and shunt resistor (section 2.2.3), rebooting of the controller which is sometimes useful and needed e. g. for firmware updates and printing the actual status of the power supply with its current settings. Most of these commands are destined to be used by the graphical user interface (GUI).

2.2.7. Output Transformer

As the final building block in this SPS the main transformer is situated before the output. Its purpose is to convert the applied power into as much current as possible. As a rule of thumb the ratio of the input and output current is indirectly proportional to the number of turns in the particular windings. As a consequence the secondary winding consists of only one turn formed by a rather thick copper strip to support the high currents. Because no special voltage ratio is desired the number of primary turns is determined by the following equation which is derived from Faraday's law, taking into account the mains voltage as well as the maximum allowed magnetic flux density of the transfomer core.

Table 2.4.: Microcontroller instruction set

Command	Description
	Discontinuous mode

`SET TEMPERATURE temp`
`SET TEMP temp`
`STE temp`
	Sets the desired boat temperature for the next firing instruction.

`SET TIME time` `STI time`	Sets the desired duration of the boat temperature during the next firing instruction.
`FIRE`	Heats the boat to the previously set temperature for the desired time.
`SET RAW DUTYCYCLE dutycycle` `SRD dutycycle`	Sets the raw value of the DAC generating the voltage used by the PWM controller for changing the duty cycle.
	Continuous mode
`POWER [ON,OFF]` `PWR [ON,OFF]`	Activates/Deactivates the power output.
`RAMP temp time`	Changes the temperature to the new value by applying a linear ramp with the specified duration.
`RAW RAMP dutycycle time` `RRAMP dutycycle time`	Varies the dutycycle to the new value through a linear ramp with the specified duration.
	Program mode
`CLEAR PROGRAM` `CLRPRG`	Clears the current program.
`START PROGRAM` `STPRG`	Executes the current program.
`PRINT PROGRAM` `PRPRG`	Returns the settings of the current program.
`PROGRAM ADD TIME time` `PRGATI time`	Adds the specific amount of time with the current temperature to the program.
`PROGRAM ADD RAMP temp time` `PRGARAMP temp time`	Adds a linear ramp of the temperature over a specified time to the program.
`PROGRAM ADD RAW RAMP dutycycle time` `PRGARRAMP dutycycle time`	Adds a linear dutycycle ramp over a specified time to the program.
`SET PROGRAM program` `SPRG program`	Sets the program according to the input string.
`SAVE PROGRAM` `SVPRG`	Saves the current program into the EEPROM.
`LOAD PROGRAM` `LDPRG`	Loads the program from the EEPROM.

Table 2.4.: Microcontroller instruction set (continued)

Command	Description
System commands	
`REBOOT` `RBT`	Reboots the controller.
`MAINPOWER [ON,OFF]` `MPWR [ON,OFF]`	Turns the main relay on/off and charges the input capacitors slowly.
`PRINT STATUS` `PRTSTAT`	Prints the current system status and settings.
`GET STATUS` `GSTAT`	Returns the raw data values via the serial port. (Used mainly by the GUI)
`SET DAC VALUE dac value` `SDV dac value`	Sets the desired DAC to a specified value.
`GET ADC VALUE adc` `GAV adc`	Returns a value from the ADC.
`SWITCH PORT number [ON,OFF]` `SWPRT number [ON,OFF]`	Switches device connected to a specified port on/off.

$$N = \frac{U \cdot t}{B_{max} \cdot A_c} \tag{2.1}$$

U	Voltage in V applied to the primary winding.
t	Maximum "on" time of a half period in s.
B_{max}	Maximum magnetic flux density of the core in T.
A_C	Core cross sectional area in m^2.

When substituting the values the equation yields:

$$N = \frac{230 \cdot \sqrt{2}\ \text{V} \cdot 1 \cdot 10^{-5}\ \text{s}}{200 \cdot 10^{-3}\ \text{T} \cdot 8.4 \cdot 10^{-4}\ \text{m}^2} = 19\ \text{Turns} \tag{2.2}$$

The core itself needs to be big enough to support all windings, it also has a saturation flux density which should not be exceeded during operation. In order to practically use the power output for connecting the TBF a mounting unit was assembled. During development it turned out that the resistance of the connection between the furnace and the power supply was crucial. As a consequence the whole transformer had to

be placed near the furnace and its secondary winding was mounted directly to the electrodes using two small brass blocks.

2.3. User Interface

Because it is not very comfortable controlling a device by typing command lines into a serial console, it was also desired to create a GUI. It should provide all the necessary features to conveniently control and reprogram the TBF with a common PC. Due to lack of time the programming of the GUI was not considered part of this thesis.

2.4. Concluding Remarks

Unfortunately the self-built power supply still had stability issues at the moment of writing this thesis. The measurements were hence carried out by using a commercial device (Agilent N8733A) able to deliver up to 220 A at a maximum of 15 V. My special thanks go to Roland Fischer, institute of inorganic chemistry, who kindly lended his power supply together with many useful ideas. It should also be noted that the secondary transformer winding had to be removed again from the furnace itself (see section 2.2.7). Nevertheless much knowledge has been gained during the developing process of the power supply project and the last version is still to come...

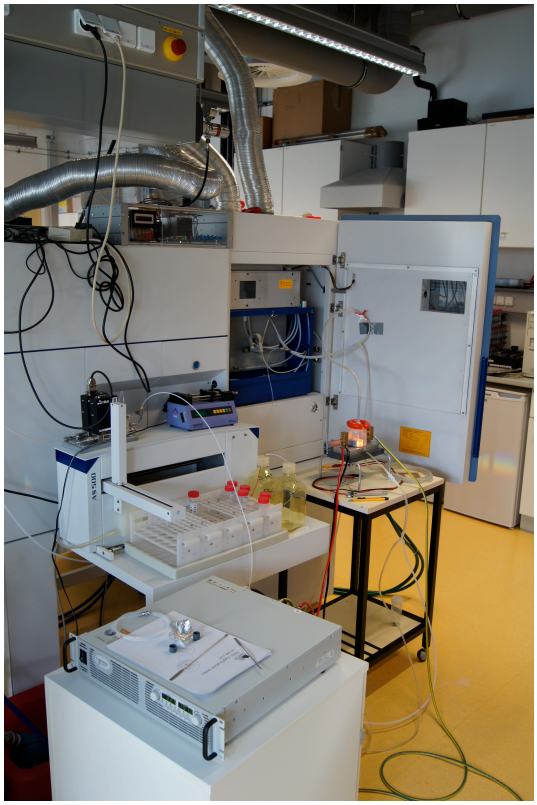

(a) At last, the whole setup in action...

(b) ... a light in the dark...

Figure 2.9.: Impressions...

CHAPTER 3

Analytical Characterization

In this chapter the experiments to determine the analytical figures of merit of the TBF are presented. The main interest was to identify the elements that vaporize and to quantify this process. Therefore a series of measurements using the ICP-OES was performed. Special interest was taken in trace elements of nickel-based steel as these alloys suffer from high spectral interference, increasing the true LODs and making the analytical process very difficult [12, 13]. That being the case, the TBF was first tested with certified reference materials (CRMs) based on a Ni-matrix. Table 3.1 lists the operating conditions of the instrument, a Spectro Ciros Vision EOP.

Due to the lack of a calibrated pyrometer it was impossible to determine the actual temperature of the tungsten boat. Instead it was tried to heat the boat to the same brightness and color each time. As an alternative the current, which should be proportional to the temperature, could be measured instead, although it should also be noted that every piece of tungsten, be it a pre-manufactured boat or a simple self-cut metal strip, has its own electrical resistance, meaning that current values therefore can only be compared while using the same metal filament in the furnace. A different boat temperature should generally result in a change of the evaporation peak shape, one of the reasons that in time resolved spectrometric measurements the peak profile is of great importance in obtaining values.

Table 3.1.: ICP-OES instrument operating conditions

Parameter	Value	Unit
Generator RF power	1400	W
Plasma gas (Ar)	12.00	L/min
Auxiliary gas (Ar)	0.60	L/min
Carrier gas (Ar)	0.83	L/min
H_2 admixed to the carrier gas stream	0.03	L/min

3.1. Tungsten Emission Spectra

The first experiments involved heating up the tungsten boat while recording emission spectra as a function of the current (and therefore the temperature). In order to avoid oxidation of the tungsten, the furnace was flushed continuously with argon gas, which in addition served as the carrier for the developing vapors. Furthermore it was reported that by adding up to 50 mL/min of hydrogen to the argon gas stream the deterioration of the tungsten boat due to oxidation can be effectively suppressed [6]. Hydrogen has a greater thermal conductivity than argon, causing the analytical zone in the plasma to become hotter which in turn leads to different excitation behavior of the electronic transitions. For that reason the spectrum shown in figure 3.1 (small part) is different with and without H_2 (blue and black curve), although an increase in hydrogen flow seems to decrease the tungsten emission again (red curve). Setting the flow too high can diminish the stability of the plasma eventually leading to extinction. Hence the subsequent experiments were all done with an additional hydrogen flow of 30 mL/min.

Tungsten is an element with many atomic and ionic emission lines (around 10000 according to [9], see also figure 3.1). As a result suitable analyte emission lines without tungsten interference had to be chosen, while the boat temperature should also be set high enough to vaporize the elements of interest but does not cause too much background from evaporated tungsten or sample matrix.

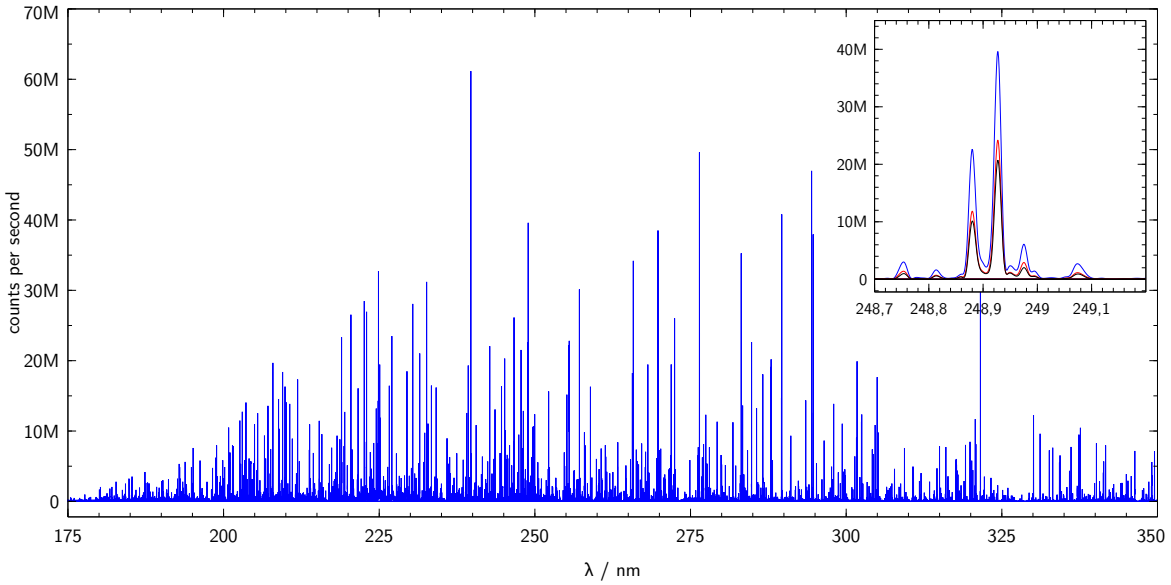

Figure 3.1.: Tungsten spectra. The small portion in the top right corner shows part of the spectrum magnified: black: without H_2, blue: with 10 mL min^{-1} H_2, red: with 30 mL min^{-1} H_2.

3.2. Time-resolved Measurements

The employed ICP-OES instrument is not well suited for time-resolved measurements, due to the slow detector read-out electronics. In order to get access to peak profiles many individual replicates were measured and evaluated afterwards in a different numerical data processing software. Although principally proportional to time the number of replicate still does not provide an accurate time scale due to the lack of the exact integration and data acquisition time.

Another peculiarity is the method used by the instrument to achieve a higher dynamic range of the detector. This is generally needed with current charge-coupled device (CCD) detector technology in order to accomplish a linear signal-to-concentration dependence over at least five orders of magnitude. The integration process is divided into five phases, each having a different integration and duration time. While the most intense signals are captured completely in a very short time (without saturating the detector), parts of the spectrum having lower intensities require longer integration times in order to attain a signal with sufficient SNR. The data from the five phases is then merged together by the manufacturer's software, achieving a greater dynamic range than would be possible with a single fixed integration time. This procedure is also known as high dynamic range (HDR) imaging. In normal steady-state measurements time is

Table 3.2.: Detector integration program

Phase	Duration s	Integration Time s
1	0.3	0.005
2	0.4	0.010
3	0.5	0.100
4	0.0	1.000
5	0.0	10.000

in fact not very important, but obviously for time-resolved measurements the total time needed for a single replicate should be rather short (in the range of one second or smaller). Since the analyte emission intensity was expected to be high because of better vaporization and sample introduction efficiency, the longest integration phases were omitted completely. After some further adaptation an approximate rate of one replicate every two seconds was achieved and considered sufficient. Besides, CCD-based signal recording can be regarded as inappropriate for high speed (> 1 Hz) time-resolved data acquisition. In [7] a PMT was used as detector instead, overcoming these limitations.

3.2.1. Calibration

Calibration in solid sampling techniques has always been challenging. Because evaporation behavior of solid samples is generally quite different to the one of liquids one would ideally use solid calibration samples, preferably with the same matrix content which is difficult to achieve for many samples. Luckily, for steel samples there is a high number of CRMs available.

Liquid Calibration

One first attempt included liquid calibration with standard solutions which were prepared using single element stock solutions. A small amount (50 µL) was dropped onto an empty tungsten boat and dried slowly. Afterwards the boat was heated up quickly, evaporating the remaining analytes.

The most obvious problem was extensive forming of blue tungsten oxide probably caused by the remaining water vapor in the furnace volume. Also the nitric acid contained in the used standard solutions was reported to oxidize the tungsten boat [5]. At higher temperatures the oxide itself evaporated and – together with elemental tungsten – provided an intense background signal. Table 3.4 gives a summary of the selected emission lines together with some comments about usability.

Even so, it was tried to create calibration data for the suitable lines. This was done by subtracting the background part of the signal and then integrating the peak area. Then a function was fitted through the obtained calibration data points. Lastly the resulting calibration data was used in an effort to determine the trace element content of a steel CRM. Section 3.2.2 describes the outcome of the steel sample evaluation.

During preparation of the multielement standard solution another problem arose. Normally single element stock solutions are prepared in nitric acid. One exception is tin which is made using hydrochloric acid to prevent forming of tin acids. When combined with a silver standard the silver precipitates as silver chloride, removing itself from the calibration solutions resulting in overestimating the silver amount in the samples (see table 3.6). This circumstance is also clearly visible in the calibration graph 3.2a as the intensity of the lowest value is disproportionally high because at low concentrations the silver has not precipitated yet, but remains in solution as colloid.

Solid Calibration

Generally the evaporation of analytes in liquid samples behaves differently than in solid samples. Therefore a better approach for calibration in direct solid sampling is to use data derived from solid sample measurements but these are often difficult to achieve and process. Ideally some CRMs are available with different amounts of the desired analytes, preferably in the same matrix. This would be called a matrix-matched calibration and is favorable because it is assumed to provide the same characteristics and behavior in the analysis as the actual sample. In this case at least two such CRMs exist and could be used to obtain calibration data and LODs (refer to section 3.2.2 and table 3.3).

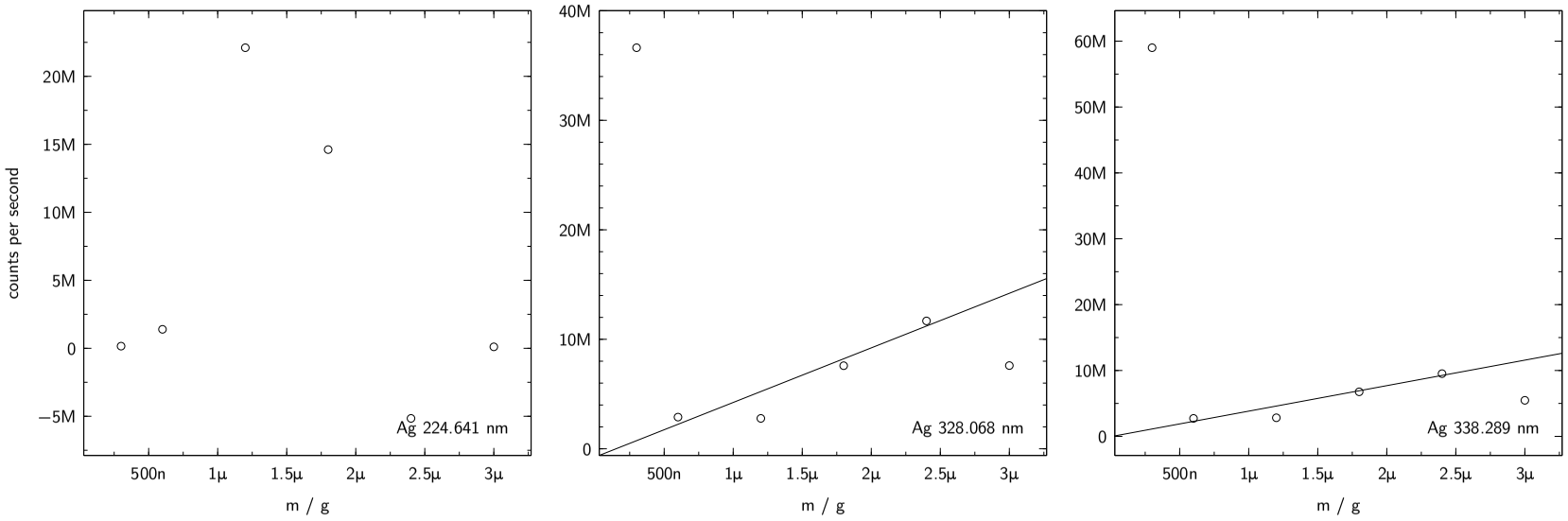

(a) Ag

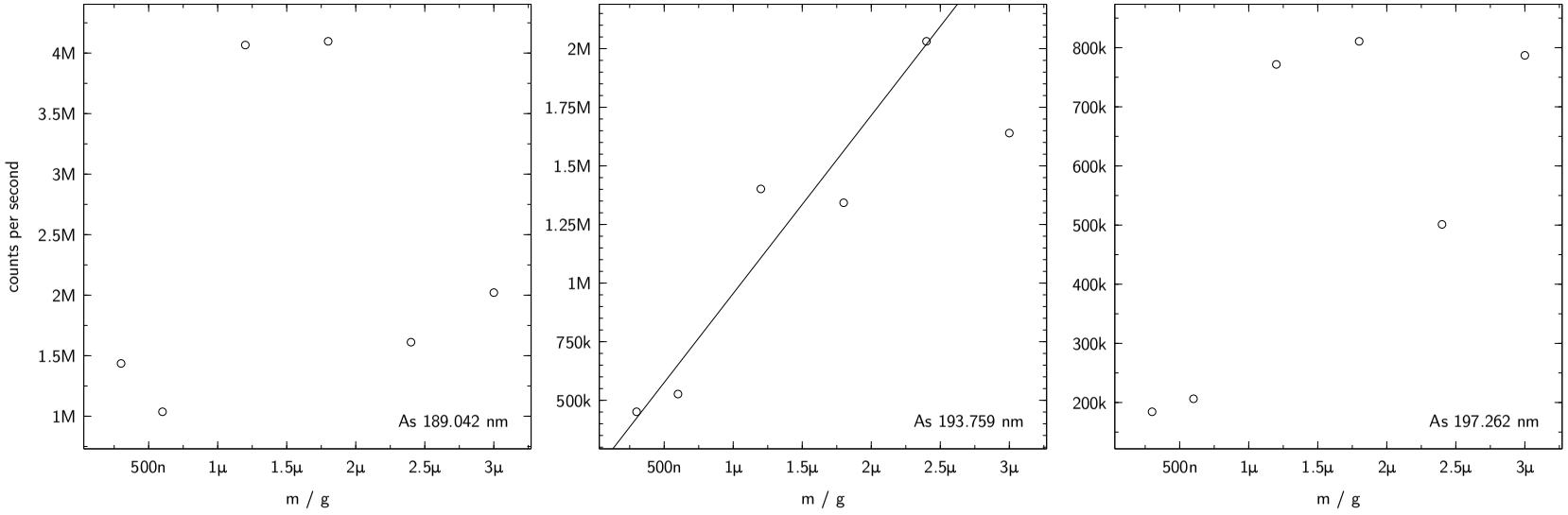

(b) As

Figure 3.2.: Liquid calibration

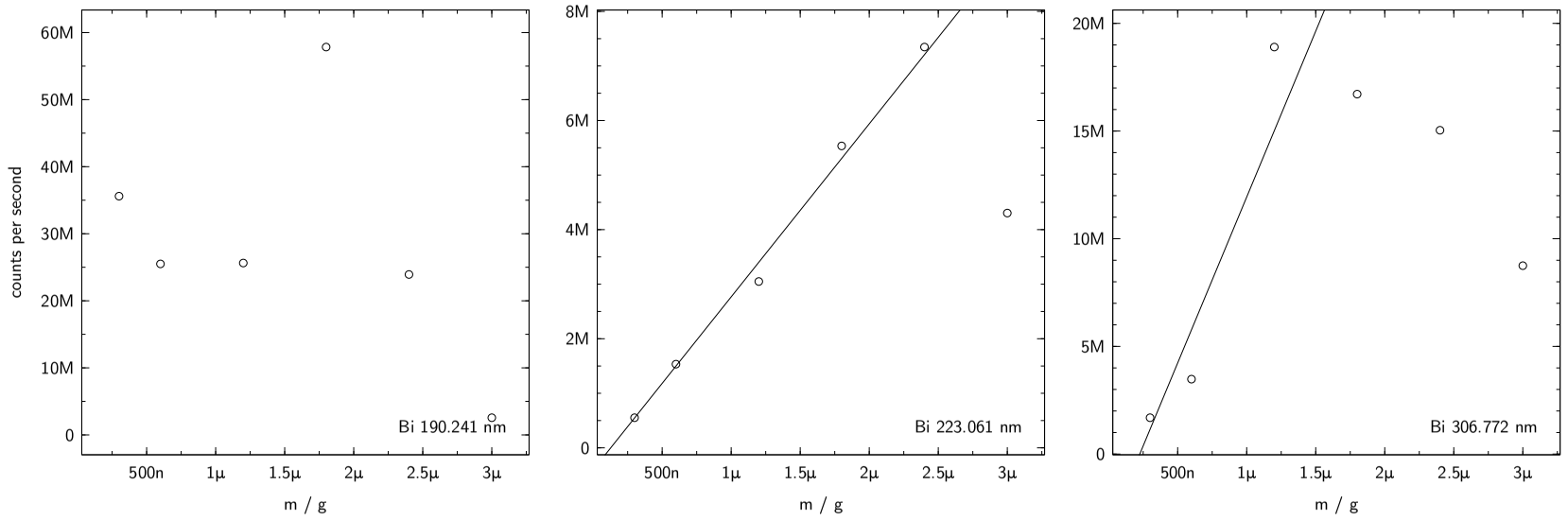

(c) Bi

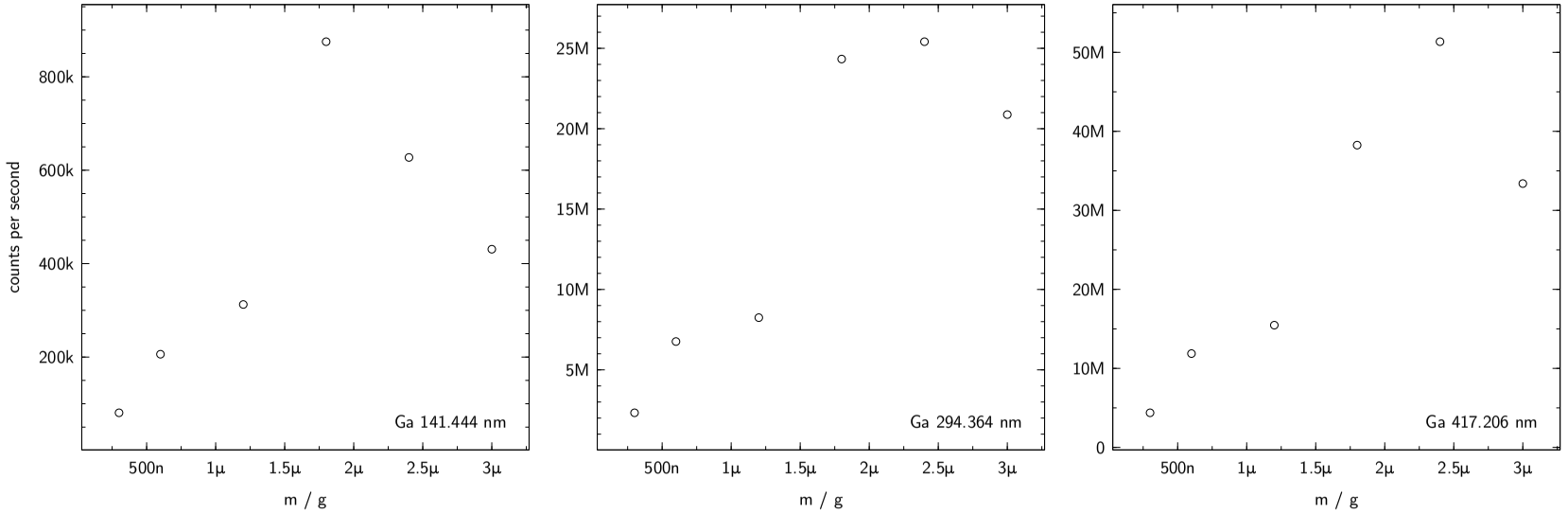

(d) Ga

Figure 3.2.: Liquid calibration (continued)

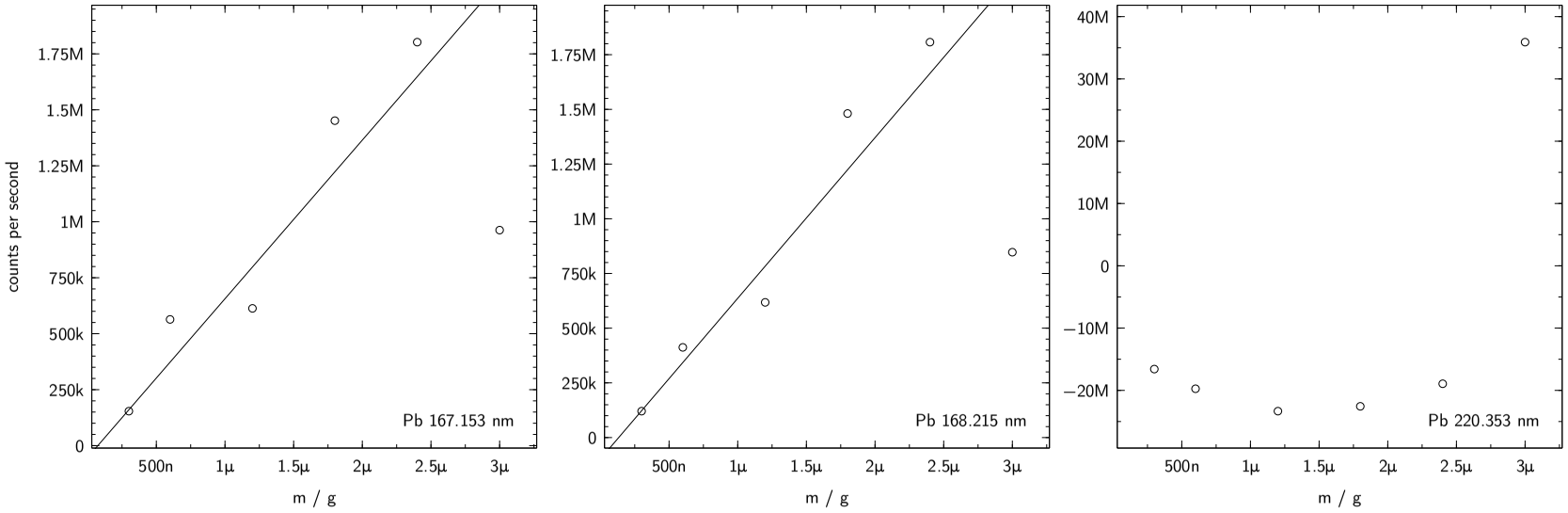

(e) Pb

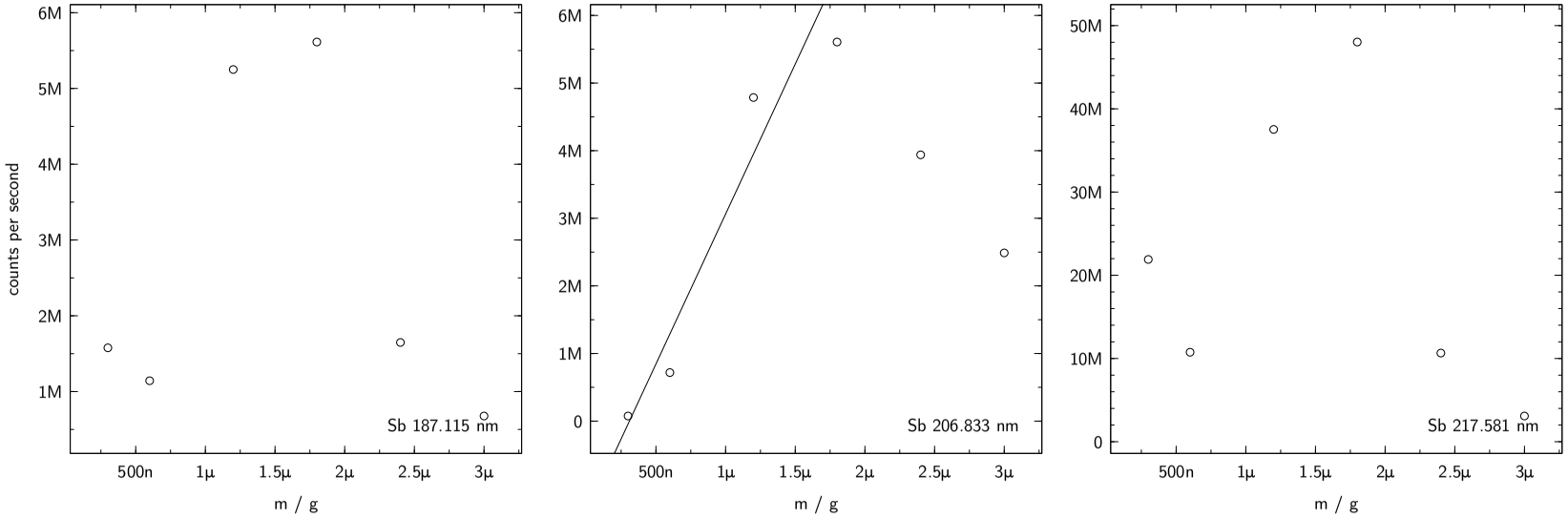

(f) Sb

Figure 3.2.: Liquid calibration (continued)

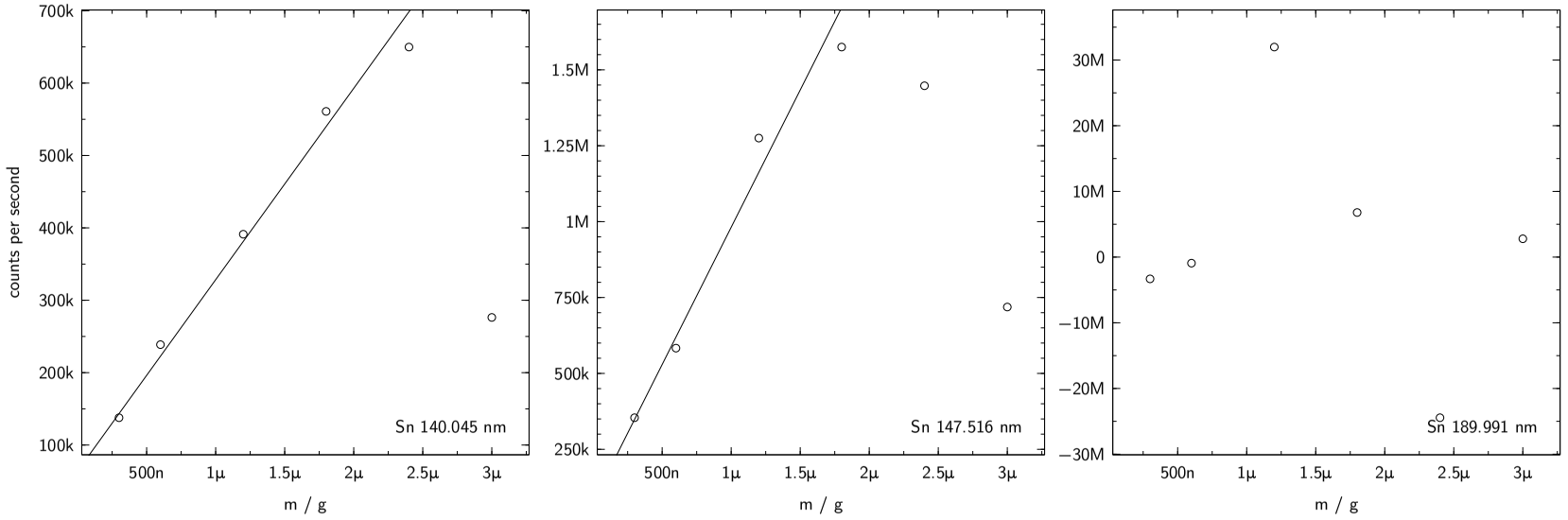

(g) Sn

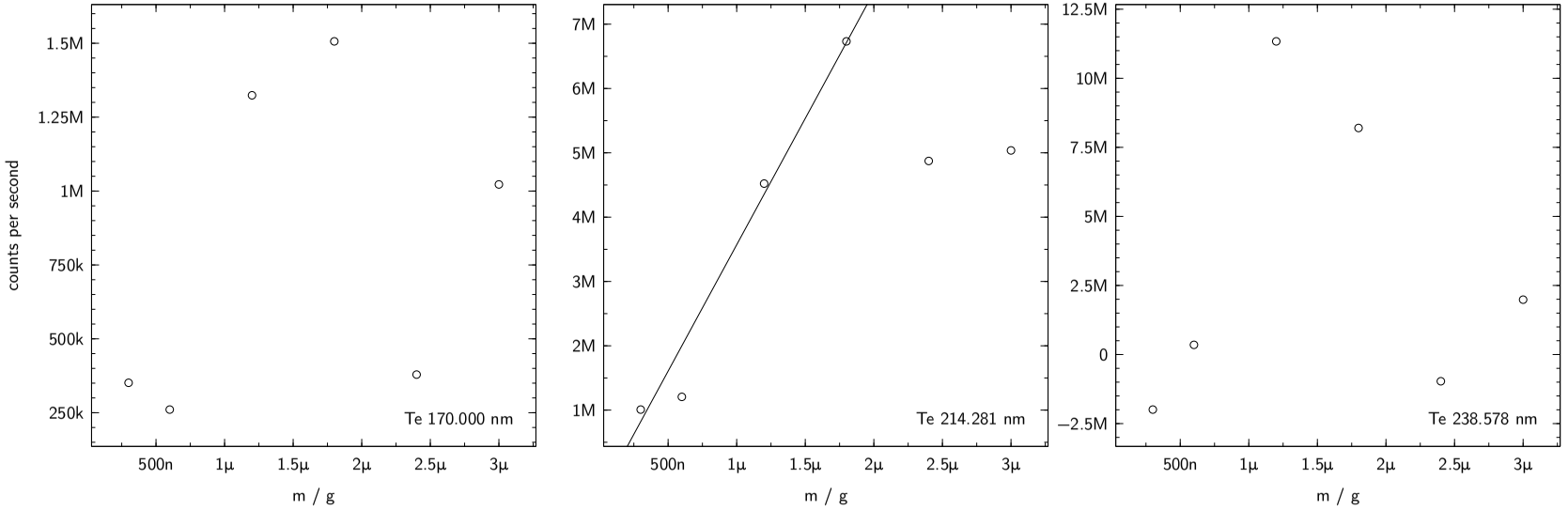

(h) Te

Figure 3.2.: Liquid calibration (continued)

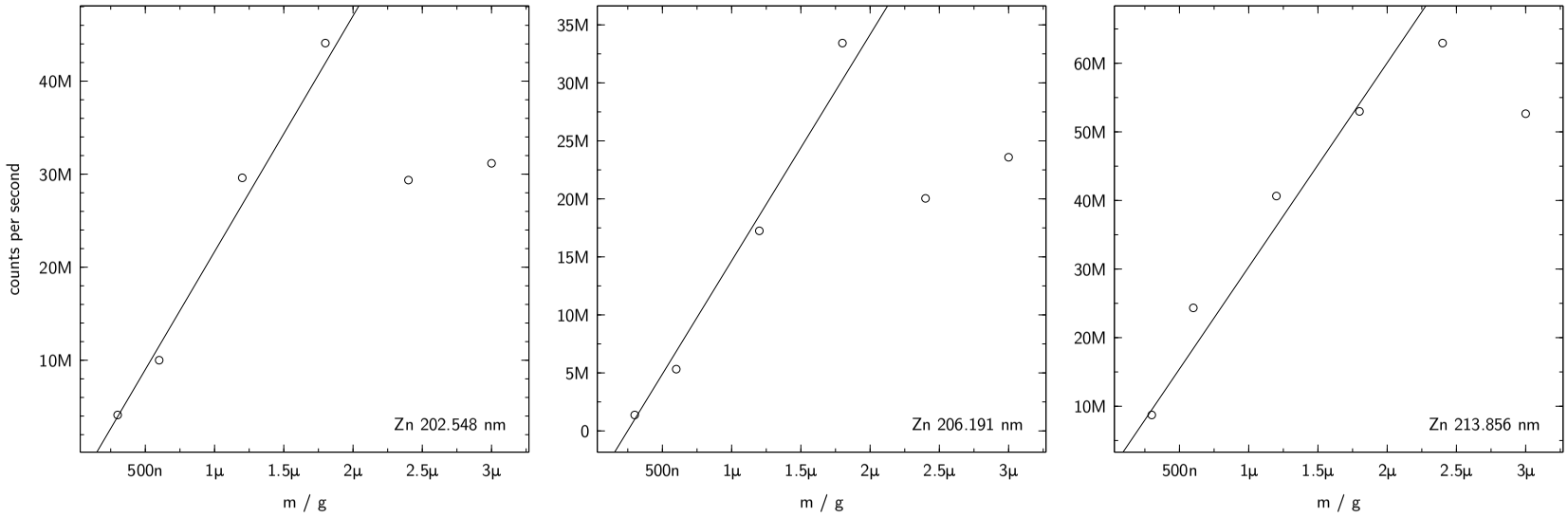

(i) Zn

Figure 3.2.: Liquid calibration (continued)

Table 3.3.: Ni-based steel CRMs with certified values in µg/g

Designation	Type	Content								
		Pb	Bi	Ag	Te	Sb	As	Ga	Sn	Zn
BCS 345	CRM	0.21	< 0.2	< 0.2	< 0.2	< 2	(2)[a]	8.2	5.6	< 0.5
BCS 346	CRM	21.0	10.4	35.0	11.7	47	50.3	50.6	91	28.9

[a] Value not certified.

3.2.2. Steel Samples

Because of special interest in this application (refer to [12] and [13]) steel samples were chosen at first, in particular CRMs based on a Ni-alloy with known values of specific trace elements (see table 3.3). Especially useful are the numbers 345 and 346 of the BCS (British Chemical Standard) series (Bureau of Analysed Samples Ltd.). BCS 345 is the basic Ni-alloy with all the main components certified while number 346 is the same base material additionally spiked with certain trace elements. Such a combination is exceptionally applicable in solid sampling techniques because it enables the meaurement of blank values as well as the analytes in a suitable concentration independently in the same matrix, thus unfolding potential blank value errors.

First Results

After completion of the apparatus the first measurements were taken with steel samples in order to get an overview of the resulting signals including potential problems like matrix and/or tungsten interference. In table 3.4 the chosen analytes of interest, their melting and boiling temperatures as well as their corresponding main emission lines are presented, while figure 3.3 shows the corresponding spectra. Figure 3.5 depicts the resulting peak profiles of the used CRM BCS 346. In addition figure 3.4 illustrates the different peak profile types encountered during the data acquisition.

Depending on the alloy, certain trace elements are more soluble than others bearing a reason for the different evaporation behavior of the analytes. For example, lead is not solved well and therefore vaporized from the molten sample more easily which is reflected in the sharper peak profile. Antimony, however, alloys better, making it

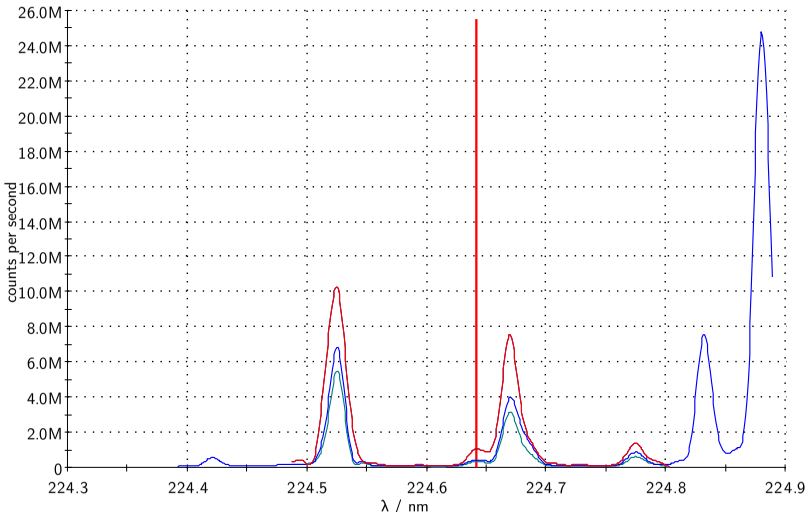

(1) Ag 224.061 nm

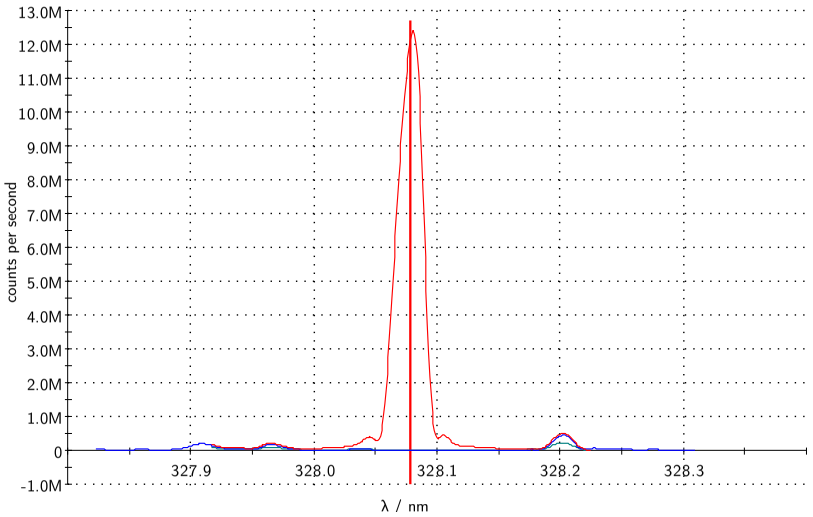

(2) Ag 328.068 nm

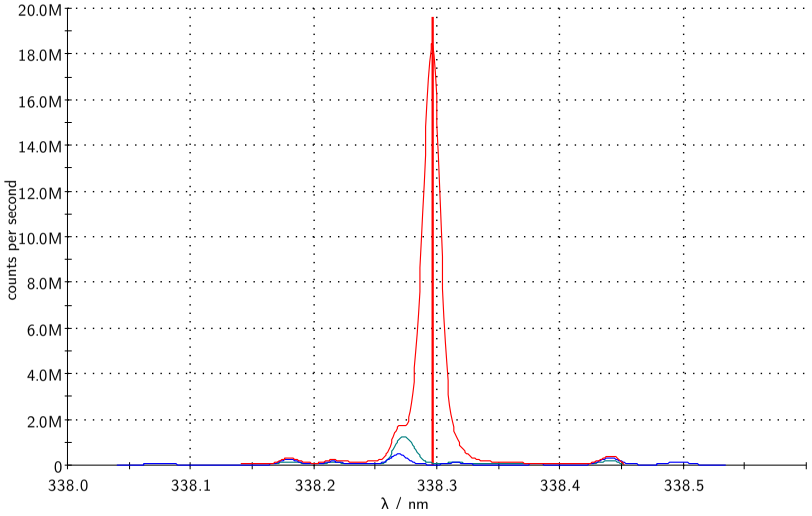

(3) Ag 338.289 nm

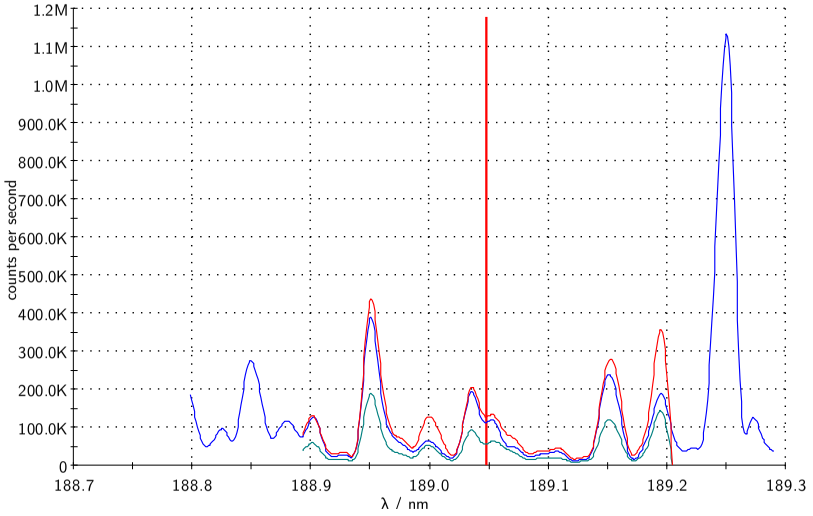

(4) As 189.042 nm

Figure 3.3.: Spectra of the chosen emission lines

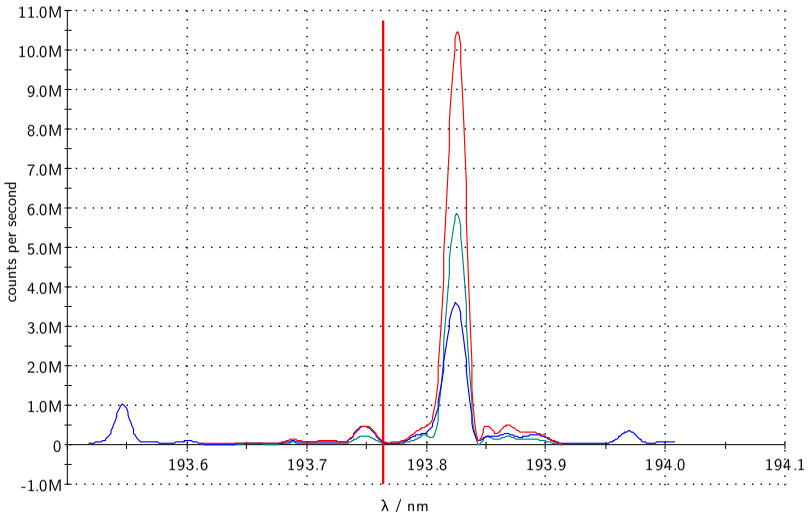

(5) As 193.759 nm

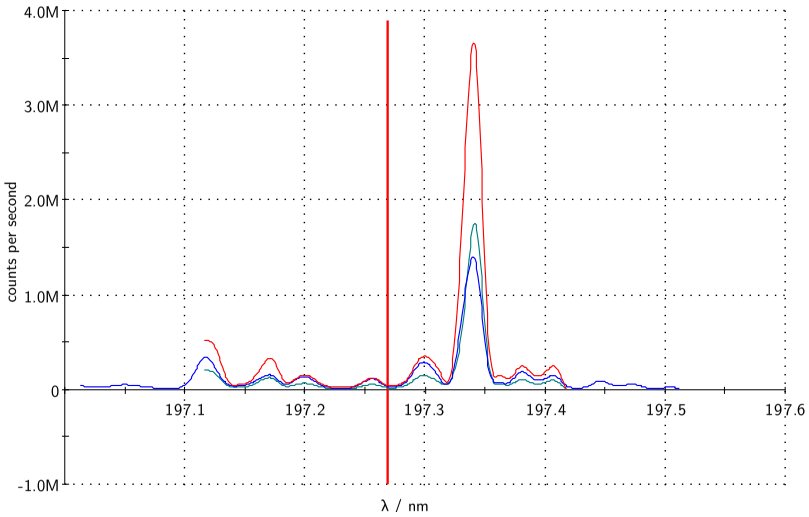

(6) As 197.262 nm

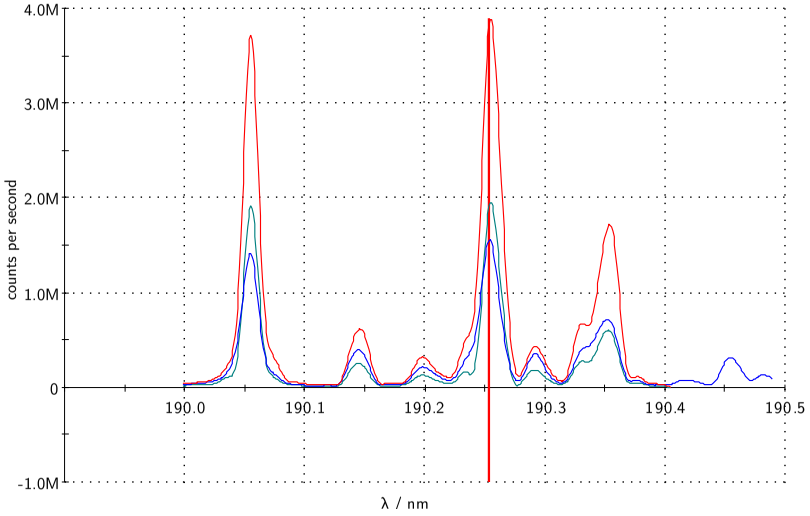

(7) Bi 190.241 nm

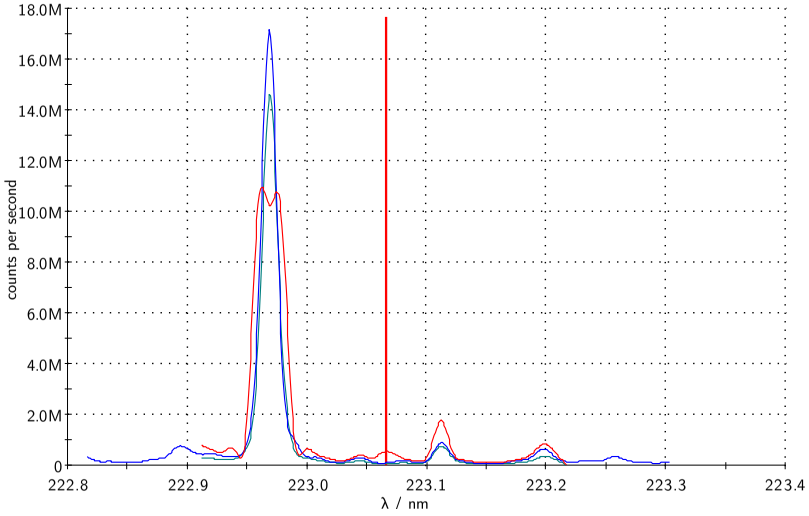

(8) Bi 223.061 nm

Figure 3.3.: Spectra of the chosen emission lines (continued)

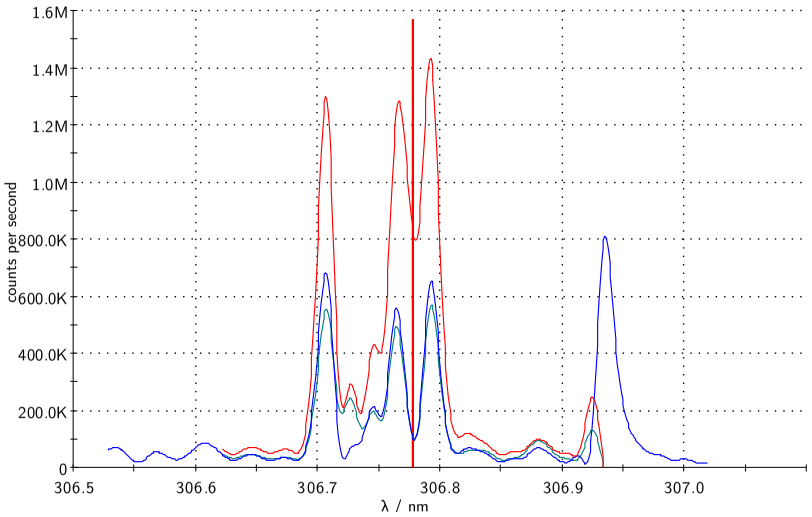

(9) Bi 306.772 nm

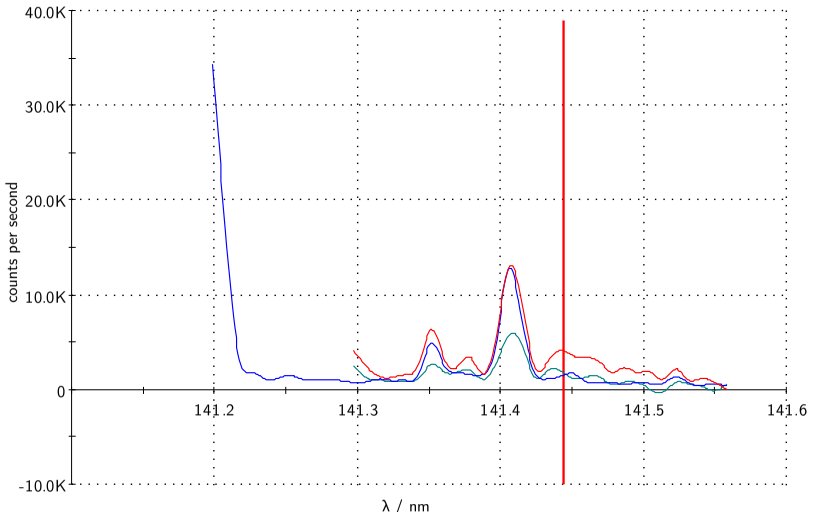

(10) Ga 141.444 nm

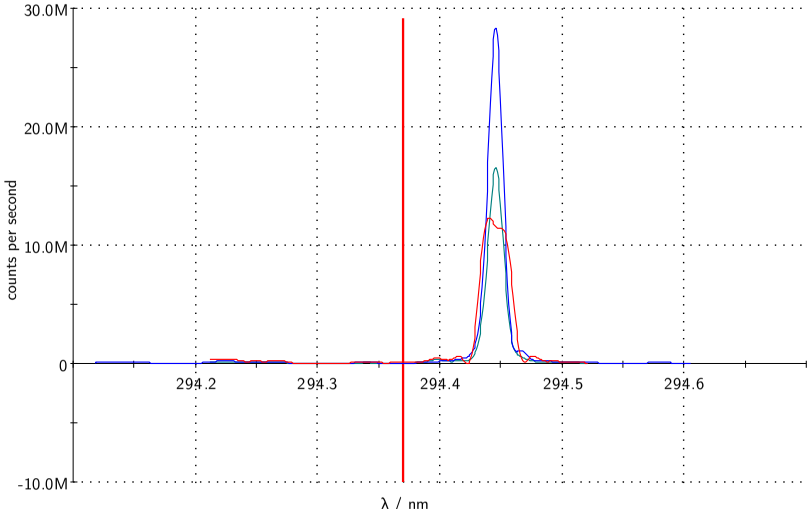

(11) Ga 294.364 nm

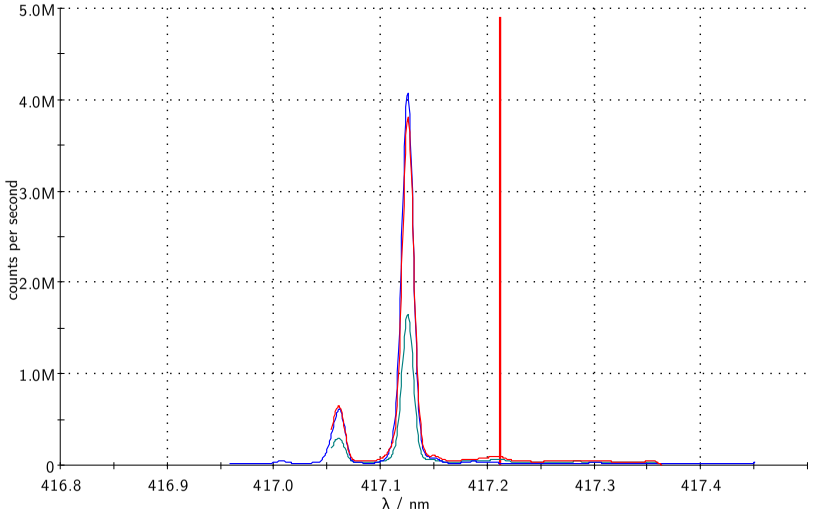

(12) Ga 417.206 nm

Figure 3.3.: Spectra of the chosen emission lines (continued)

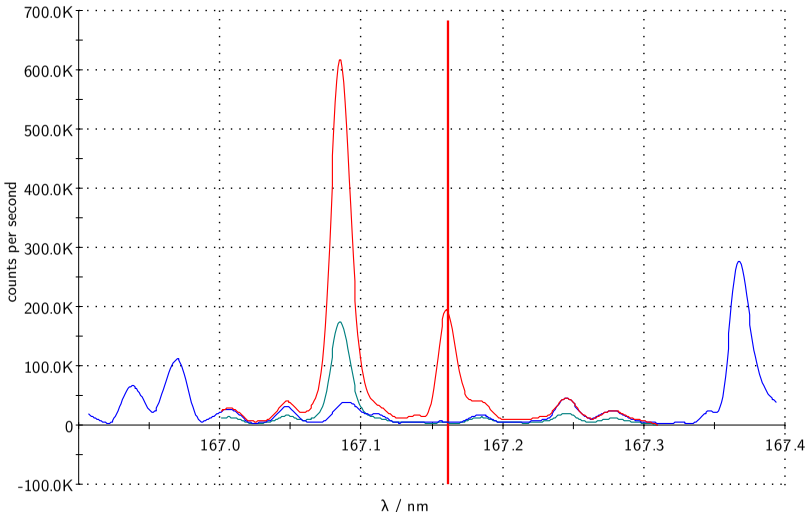

(13) Pb 167.153 nm

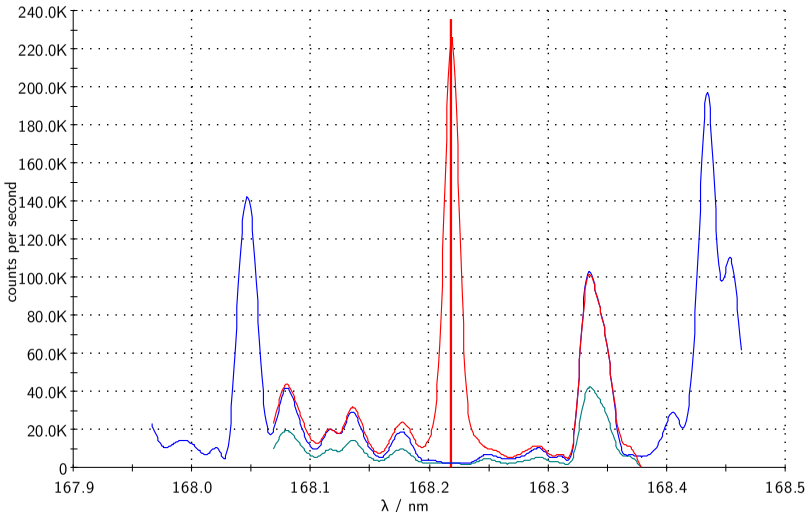

(14) Pb 168.215 nm

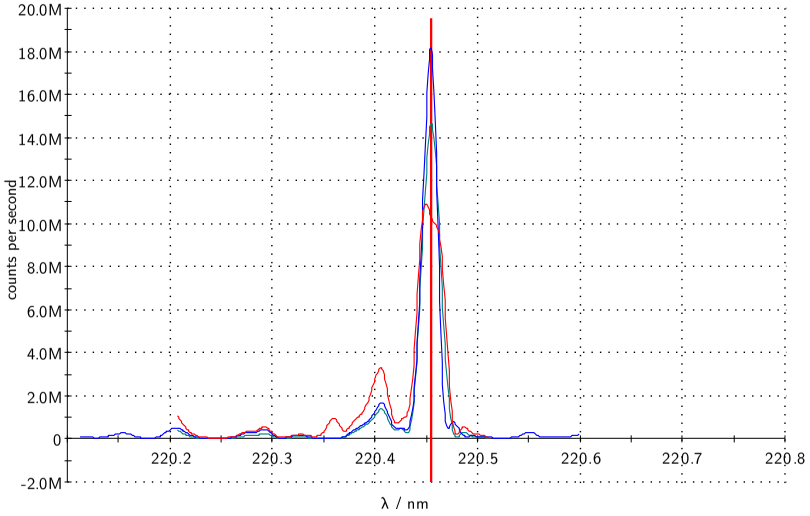

(15) Pb 220.353 nm

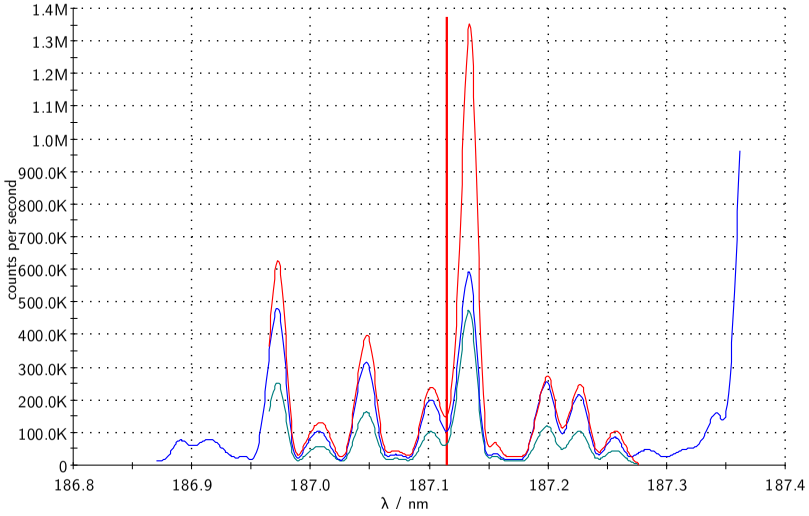

(16) Sb 187.115 nm

Figure 3.3.: Spectra of the chosen emission lines (continued)

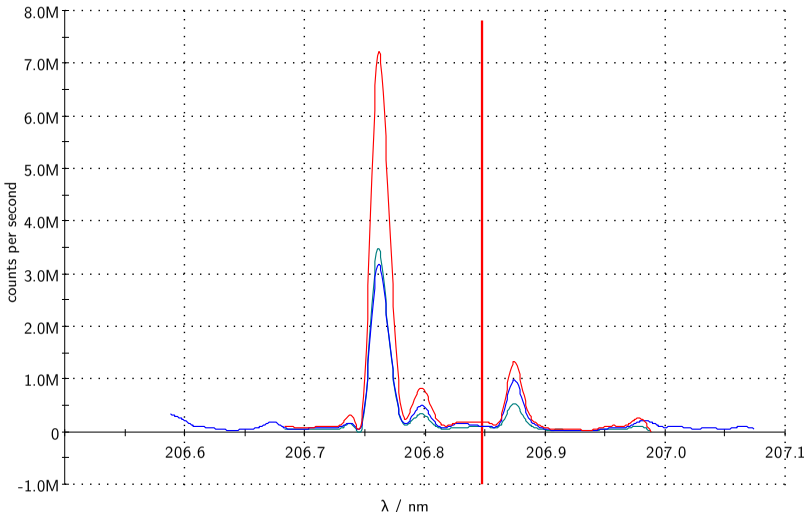

(17) Sb 206.833 nm

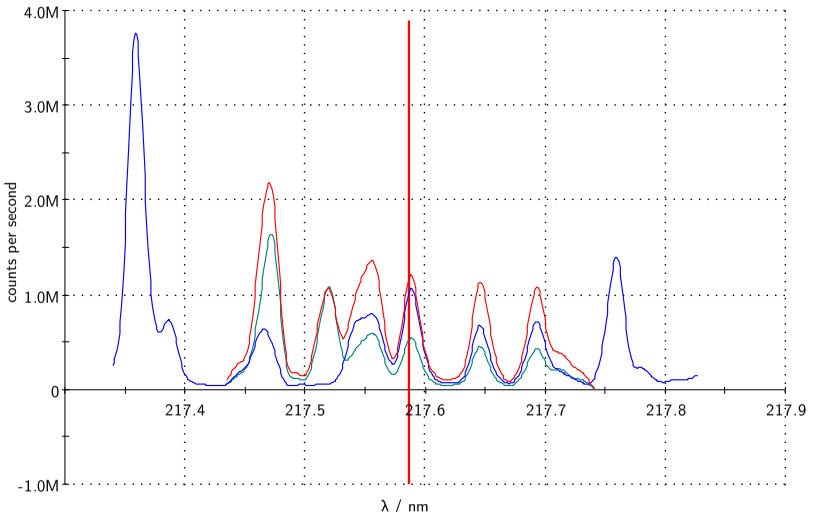

(18) Sb 217.581 nm

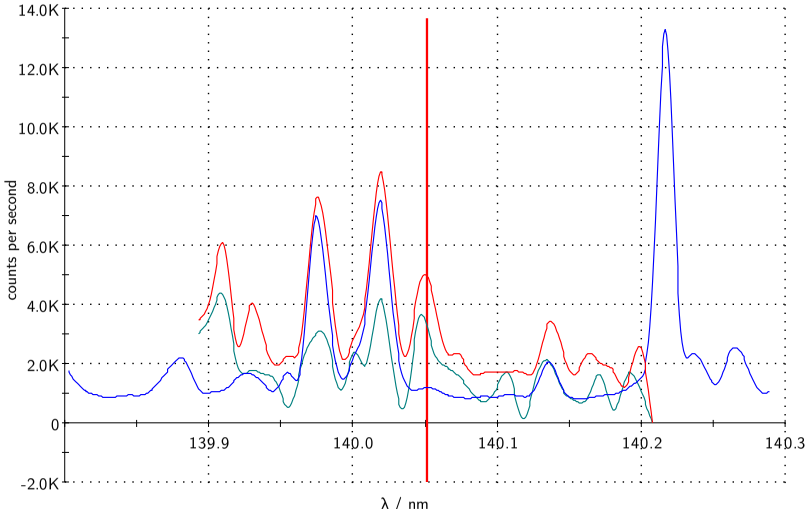

(19) Sn 140.045 nm

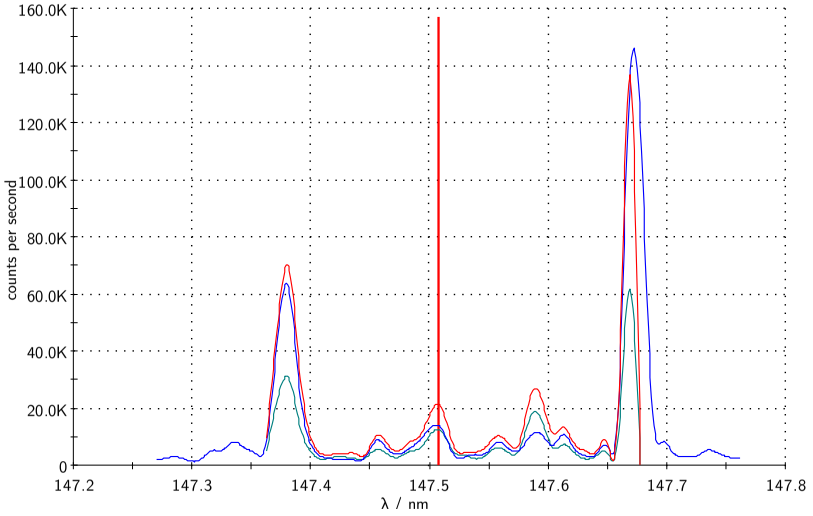

(20) Sn 147.516 nm

Figure 3.3.: Spectra of the chosen emission lines (continued)

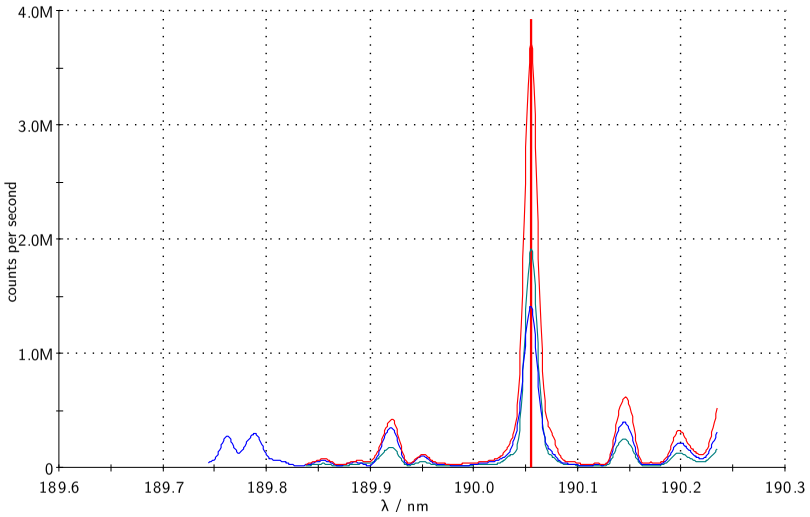

(21) Sn 189.991 nm

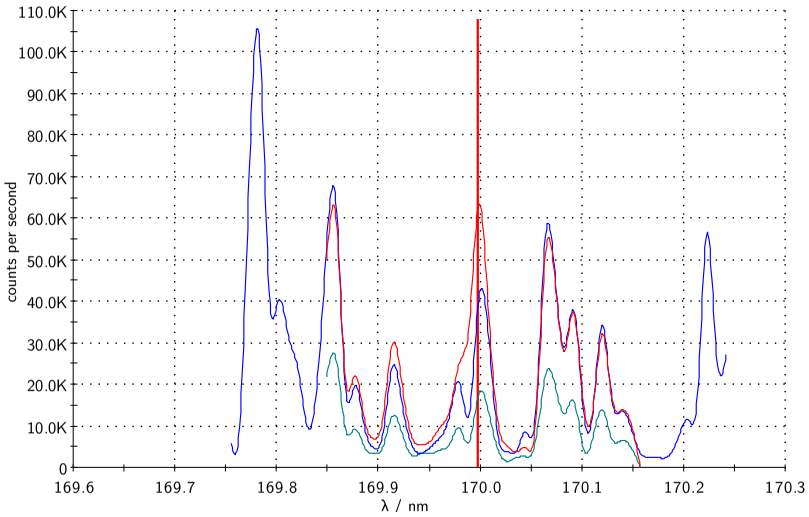

(22) Te 170.000 nm

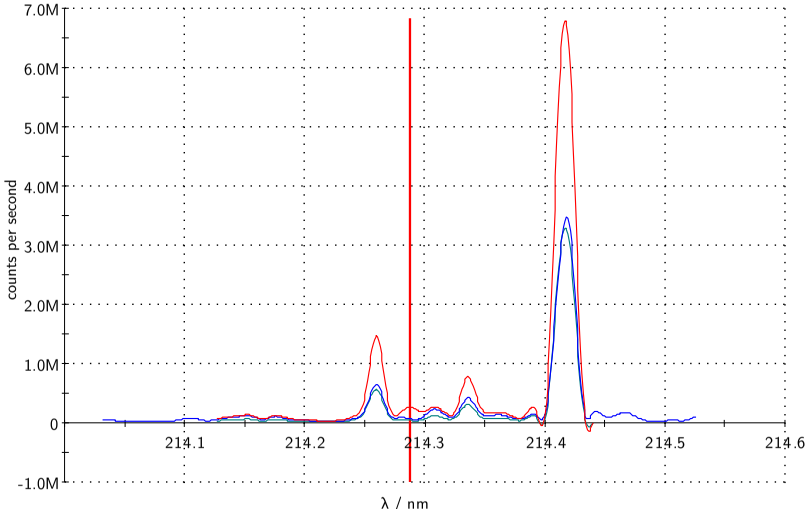

(23) Te 214.281 nm

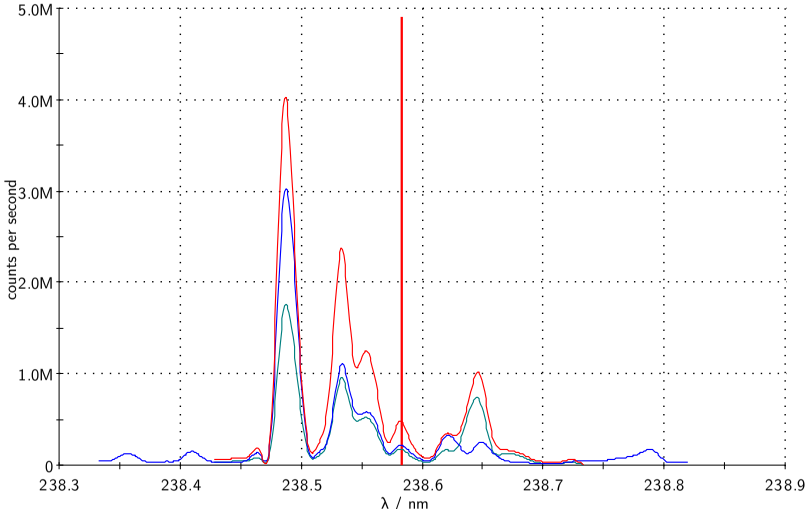

(24) Te 238.578 nm

Figure 3.3.: Spectra of the chosen emission lines (continued)

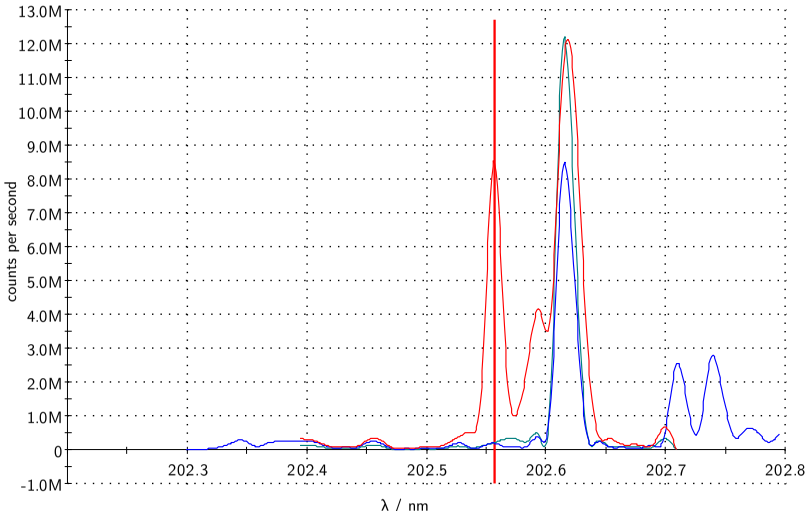

(25) Zn 202.548 nm

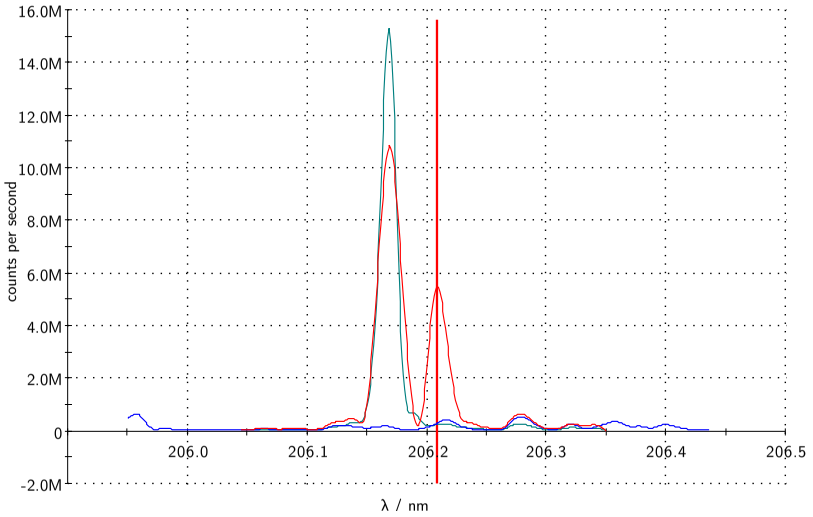

(26) Zn 206.191 nm

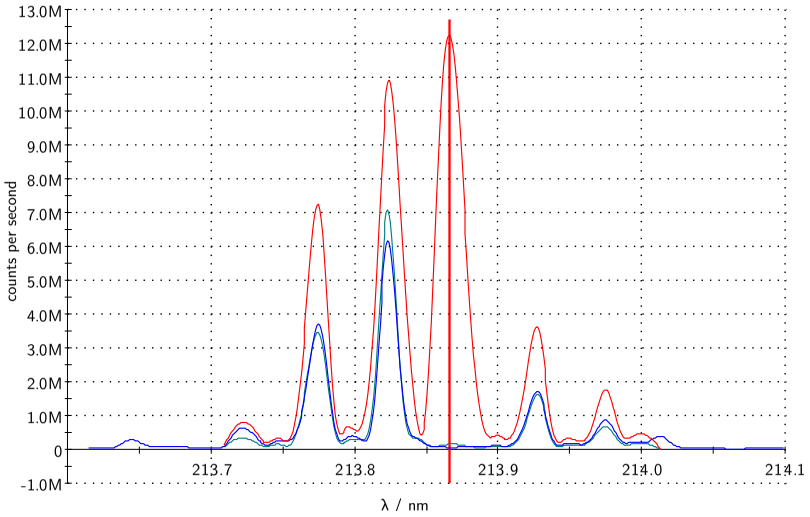

(27) Zn 213.856 nm

Figure 3.3.: Spectra of the chosen emission lines (continued).

The thick red line marks the monitored wavelength, the colors of the curves represent the following spectra: red: sample signal, blue: tungsten background, cyan: sample signal at the end of evaporation. It should be noted that the observed wavelength had to be adjusted slightly. The difference to the nominal ones is due to instrument specific wavelength deviation.

Notes:

In spectrum 15 a wrong line was selected. Left to the main wavelength in spectrum 26 a possible chromium-interference (206.149 nm) is visible.

Table 3.4.: Melting (T_m) and boiling points (T_b) of the elements [1] as well as the chosen wavelengths

Element	T_m °C	T_b °C	Line Type	Wavelength nm	Remarks
Ag	961.78	2162	Ag II	224.641	very weak
			Ag I	328.068	usable
			Ag I	338.289	usable
As	817 (t)[a]	614 (s)[b]	As I	189.042	interference
			As I	193.759	very weak, interference
			As I	197.262	very weak, interference
Bi	271.40	1564	Bi II	190.241	strong interference
			Bi I	223.061	usable, weak
			Bi I	306.772	usable, interference
Ga	29.76	2204	Ga II	141.444	low SNR
			Ga I	294.364	usable, T_b too high
			Ga I	417.206	usable, T_b too high
Pb	327.46	1749	Pb II	167.153	usable
			Pb II	168.215	usable
			Pb II	220.353	wrong line selection
Sb	630.63	1587	Sb I	187.115	interference
			Sb I	206.833	weak signal
			Sb I	217.581	interference
Sn	231.93	2602	Sn II	140.045	usable, T_b too high, weak signal
			Sn II	147.516	usable, T_b too high, weak signal, interference
			Sn II	189.991	strong interference
Te	449.51	988	Te I	170.000	usable, weak signal, interference
			Te I	214.281	usable, weak signal
			Te I	238.578	interference
Zn	419.53	907	Zn II	202.548	usable
			Zn II	206.191	usable
			Zn I	213.856	usable
Ni	1455	2913	–	–	major components of alloy
Co	1495	2927	–	–	
Cr	1907	2671	–	–	
W	3422	5555	–	–	–

[a] triple point
[b] sublimation temperature

difficult to release. Further discussion is closely related to the field of metallurgy and considered out of the scope of this work.

In the following list a short qualitative description of the information gained from this first attempt is given.

Ag Very good profile; two lines of satisfactory intensity
As Spectral interference; partly weak signals
Bi Good signal; possible tungsten interference or long tailing; both lines usable
Ga Signal, but boiling point probalby too high for complete evaporation
Pb Acceptable peak profile; good SNR but possible detector saturation
Sb Spectral interferences
Sn Weak signal; low SNR; possible interference with tungsten; boiling point maybe too high for evaporation
Te Peak of rather low intensity; long tailing or tungsten interference
Zn Good peak profile; high sensitivity

Final Evaluation

The final experiments were designed to observe if the analytes can be vaporized from the matrix completely and if the tungsten boat can be reused despite the remainder from previous samples. In order to investigate the first question, about 30 mg of the BCS 346 CRM were loaded onto a fresh boat and heated up three times in a row. The form of the signals was similar to the first measurements and it appeared that after the first heating-up no further signal from the analytes occurred (see figure 3.6). Thus it was evident that no further evaporation is happening and seemingly complete vaporization is feasible with an appropriate boat temperature.

Finally it was of interest if and how many times the boat can be used sequently. For this purpose the BCS 345 material was loaded three times followed by two samples of BCS 346. The last heating-up had to be aborted because the sample did not melt completely anymore. Due to the remains of the previous samples the mass of the boat had been increased, thus needing more power and time to heat up. It was not determinable if a tungsten-nickel-alloy or just a superficial junction between the tungsten boat and the sample matrix had been formed (see also figures 4.1 and 4.2), since such compounds are

(a) Complete evaporation of the analyte occurs, almost no tailing is visible. This is the desired peak form as the area can easily computed because the peak limits are clearly visible while a sufficient SNR is maintained.

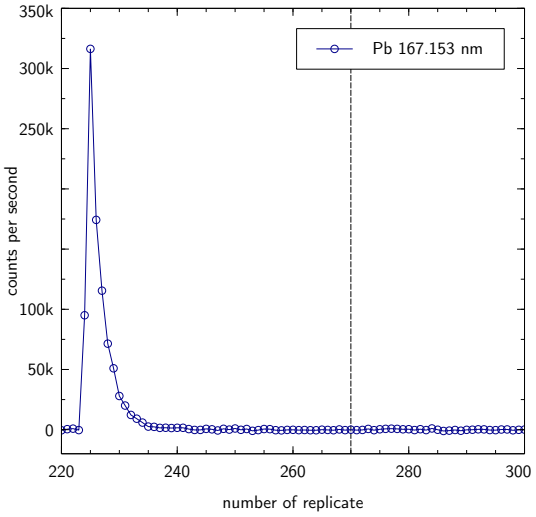

(b) Boiling temperature of the element is too high for evaporation, the peak shows a long tail signifying still ongoing vaporization until the end of the heating process (marked by the dotted line at replicate 270). Part of the analyte remains in the sample leading to an underestimation of analyte content.

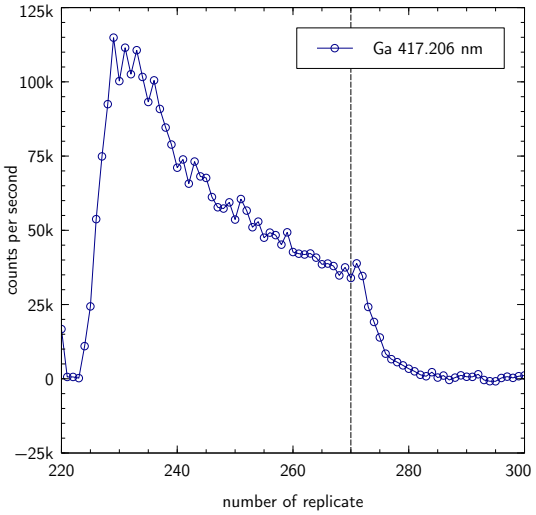

(c) Partial spectral interference. The desired peak exists with sufficient slope but towards the end of the heating period some noise persists at a nearly fixed level. With some underground correction values can possibly be extracted from this type of signal even though the cause of the noise should be investigated separately. At the end of the heating phase a small peak is visible (replicate 271), it is probably caused by gas dynamic effects and occurs in all measurements.

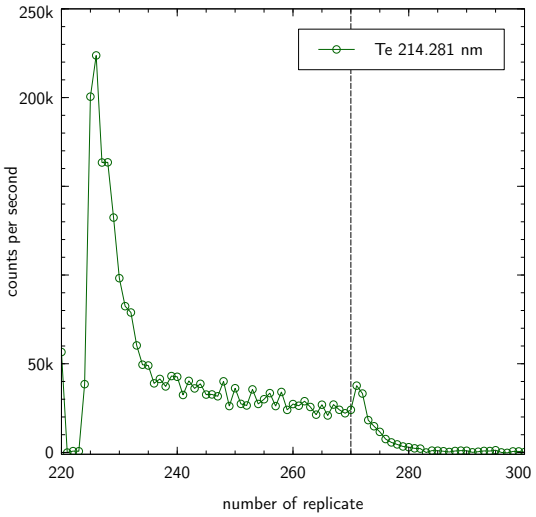

Figure 3.4.: Peak profile types. The dotted line marks the end of the heating process.

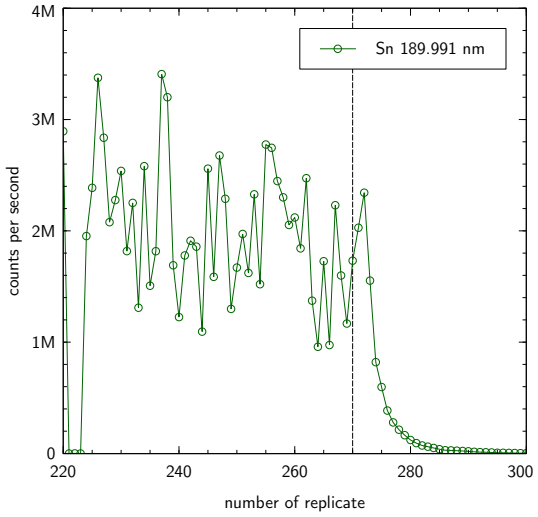

(d) Spectral interference. Although the magnitude is in the range of megacounts per second the signal merely consists of noise-like data and is therefore not evaluable. Possible explanation is an interference with some other atomic emission line, most likely from tungsten or other matrix components.

Figure 3.4.: Peak profile types (continued)

Table 3.5.: Summary of analyzed samples

Sample ID	Material	Weight mg	Remarks
1	BCS 346	27.5	first evaluation, see figure 3.5
2	BCS 346	30.9	complete evaporation test, see figure 3.6
3	BCS 346	30.0	boat usability test, see figure 3.7
4	BCS 346	35.8	boat usability test, see figure 3.7

easily generated with tungsten (refer to [3, pp. 43-50] and figure 1.7). It was evident that the boat could not be heated to a sufficient temperature anymore. The shape of the signal profiles also became broader and even distorted, suggesting further influence of the previously applied samples on the vaporization conditions.

All these measurements were used together with the liquid calibration data to determine and verify the analyte concentrations in the steel samples. LODs were extracted from BCS 345 samples by taking three times the standard deviations of the intensities and converting them into concentrations using the known certified values provided for the BCS 346 material [4]. Tables 3.5 and 3.6 contain the description of all used measurements and the calculated values respectively.

As mentioned before silver values are erroneously high due to precipitation of AgCl in the calibration solutions. In the last experiment (figure 3.7) which consisted in trying to load the boat with multiple samples in a row, the second BCS 346 sample did not

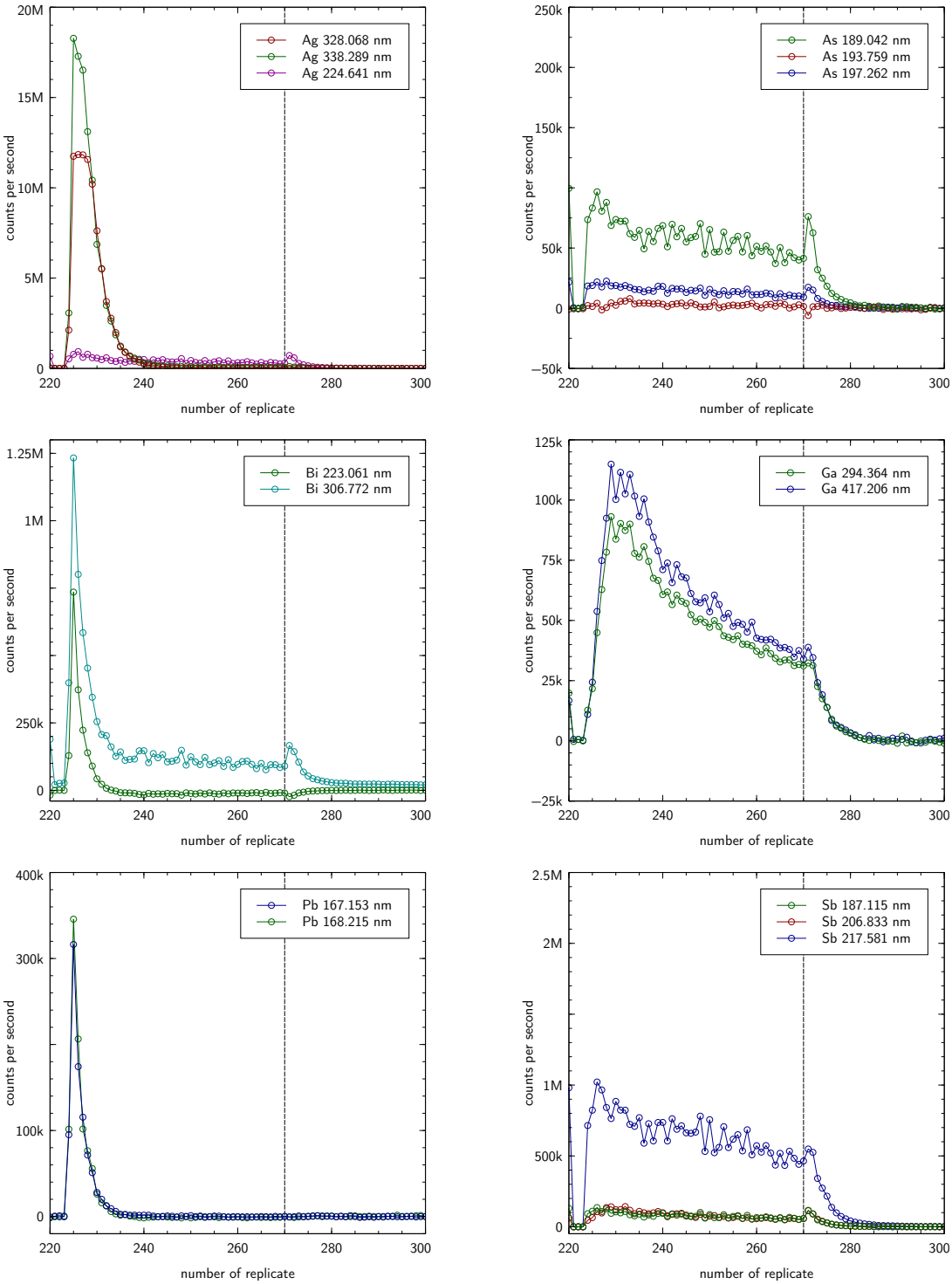

Figure 3.5.: Peak profiles of selected lines

Table 3.6.: Summary of analysis results

Element	Line	Certified	BCS 346				LOD[e]	LA-LOD[f]
			1	2	3[c]	4[d]		
	nm	µg/g	µg/g	µg/g	µg/g	µg/g	µg/g	µg/g
Ag[b]	328.068	35.0 ± 1.0	606	517	570	197	0.002	0.008
	338.289		923	856	726	238	0.01	
Bi	223.061	10.4 ± 0.4	25.9	21.6	14.6	15.1	0.02	0.002
	306.772		14.8	11.5	10.7	9.09	0.005	
Ga[a]	141.444	50.6 ± 1.4	–	–	–	–	–	0.006
	294.364		–	–	–	–	–	
	417.206		–	–	–	–	–	
Pb	167.153	21.0 ± 1.0	45.1	42.8	30.0	26.2	0.2	0.008
	168.215		49.1	30.2	23.7	22.4	0.4	
Sb	206.833	47 ± 4	–	–	–	–	–	0.006
	217.581		–	–	–	–	–	
Sn[a]	140.045	91 ± 8	–	–	–	–	–	0.006
	147.516		–	–	–	–	–	
Te	170.000	11.7 ± 1.0	7.66	4.31	5.51	2.74	1	0.07
	214.281		13.7	10.7	11.0	5.98	0.04	
Zn	202.548	28.9 ± 1.6	55.7	22.3	13.4	17.7	0.1	0.06
	206.191		51.3	22.9	17.0	18.6	0.2	
	213.856		80.7	56.7	24.4	39.2	0.04	

[a] Boiling temperature probably too high for complete evaporation.

[b] Silver precipitated in standard solutions, therefore values are too high.

[c] Boat was loaded with BCS 345 before (three times), it did not reach the same temperature.

[d] Due to the remains from previous measurements the sample did not melt completely.

[e] LODs are valid for a sample weight of about 30 mg.

[f] LODs taken from [11] for comparison.

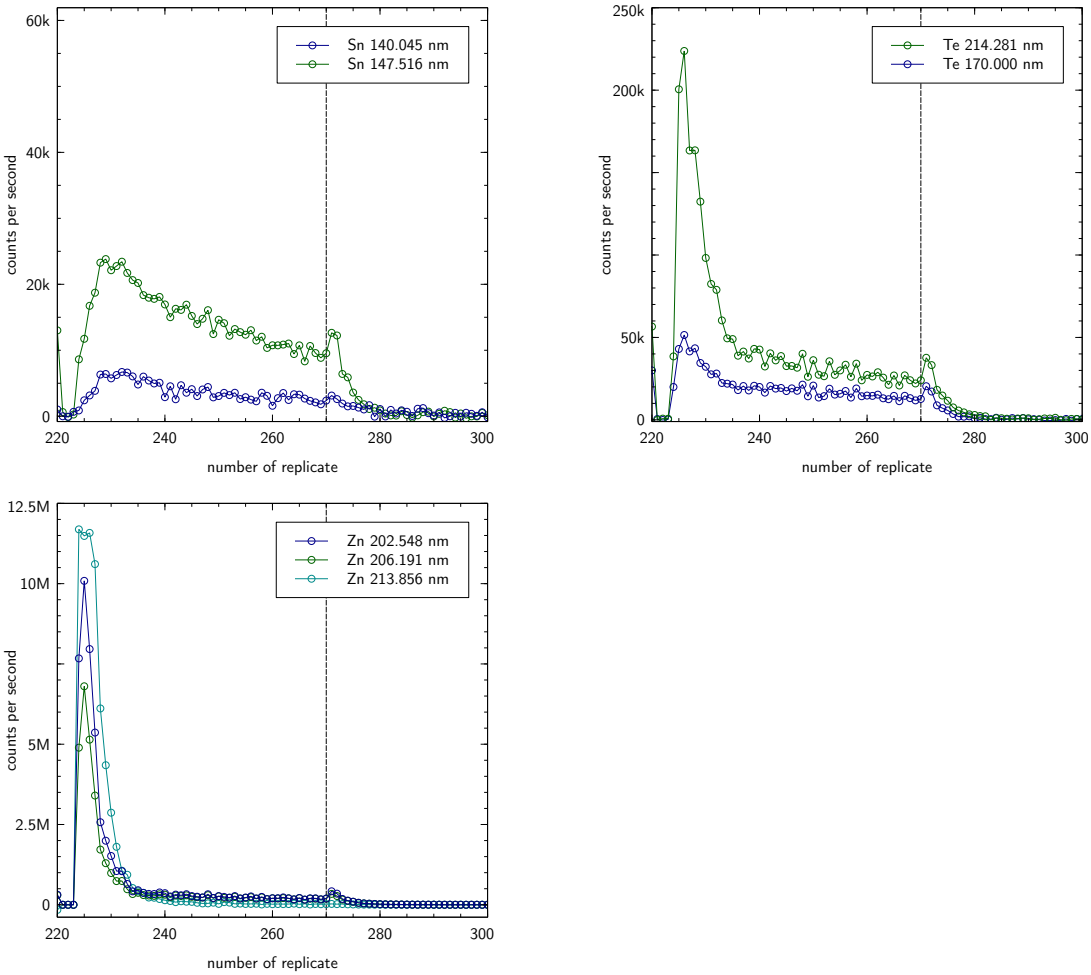

Figure 3.5.: Peak profiles of selected lines (continued)

melt completely and even the one before had already distorted signals resulting in an apparent lower content for both of them. Even so the obtained values appear to be in the same order of magnitude, although the certified content of the CRMs was not reached. Also reproducibility seems very modest at the moment, most likely due to poorly controlled operating conditions. The LODs – when available – are relatively similar to the ones accomplished in LA but at significantly reduced equipment costs.

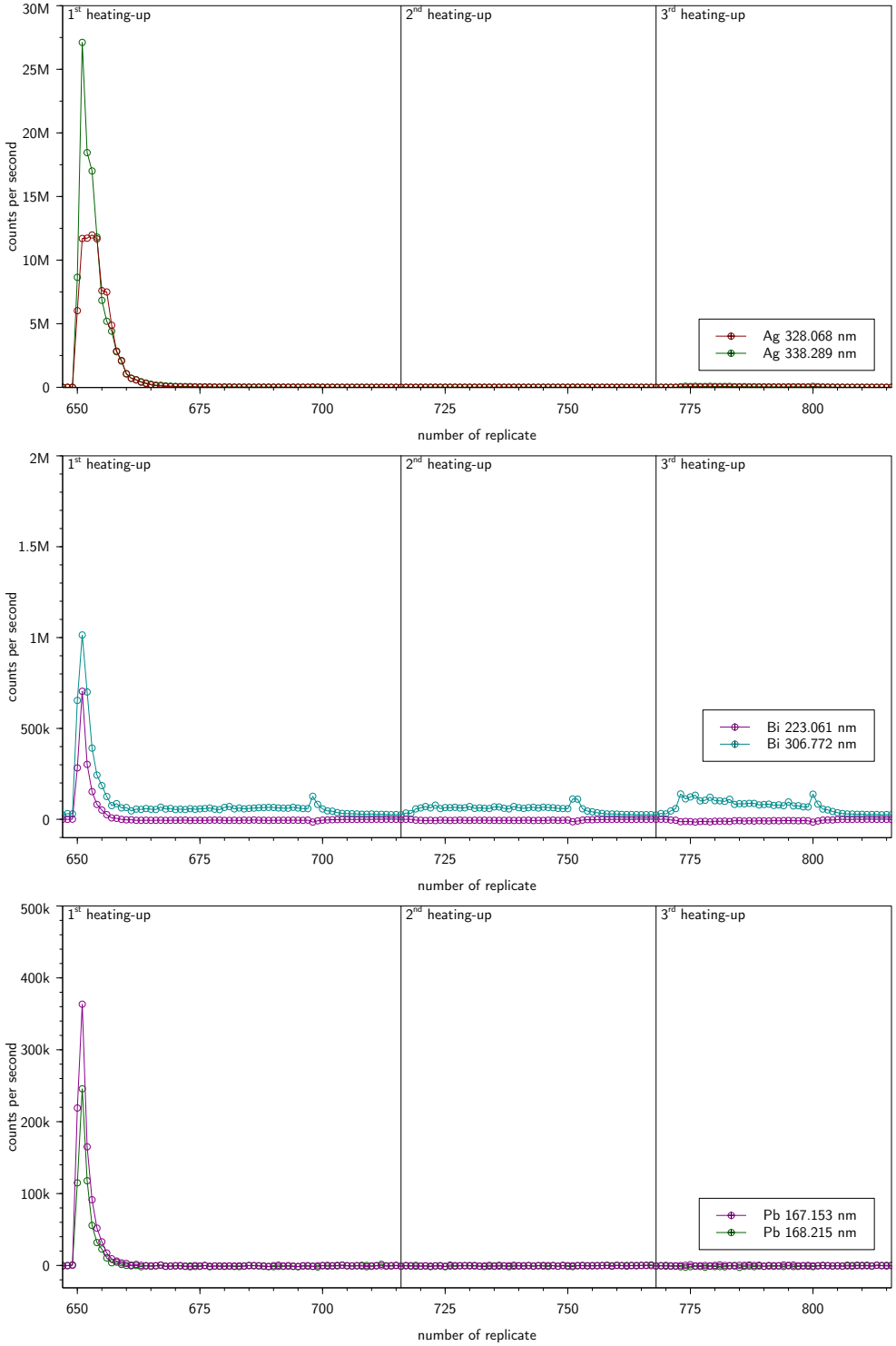

Figure 3.6.: BCS 346 sample heated up three times in a row on the same boat

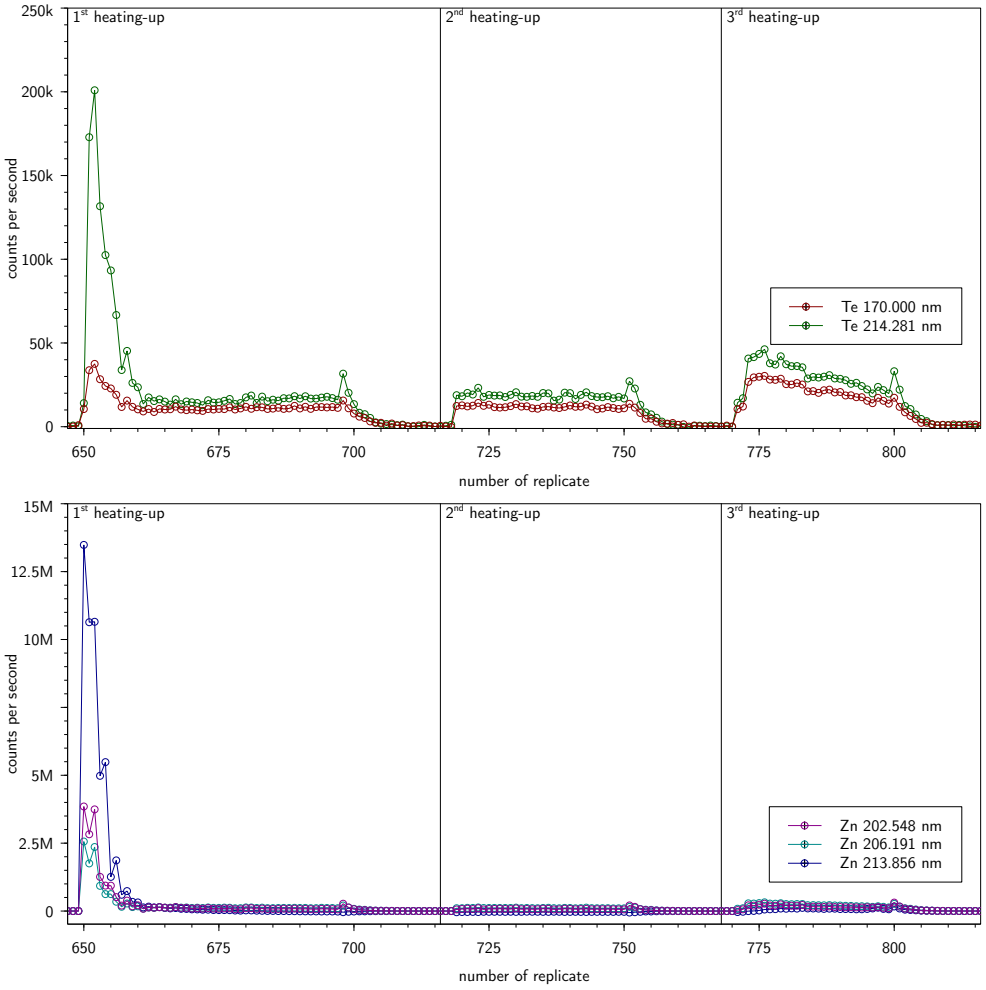

Figure 3.6.: BCS 346 sample heated up three times in a row on the same boat (continued)

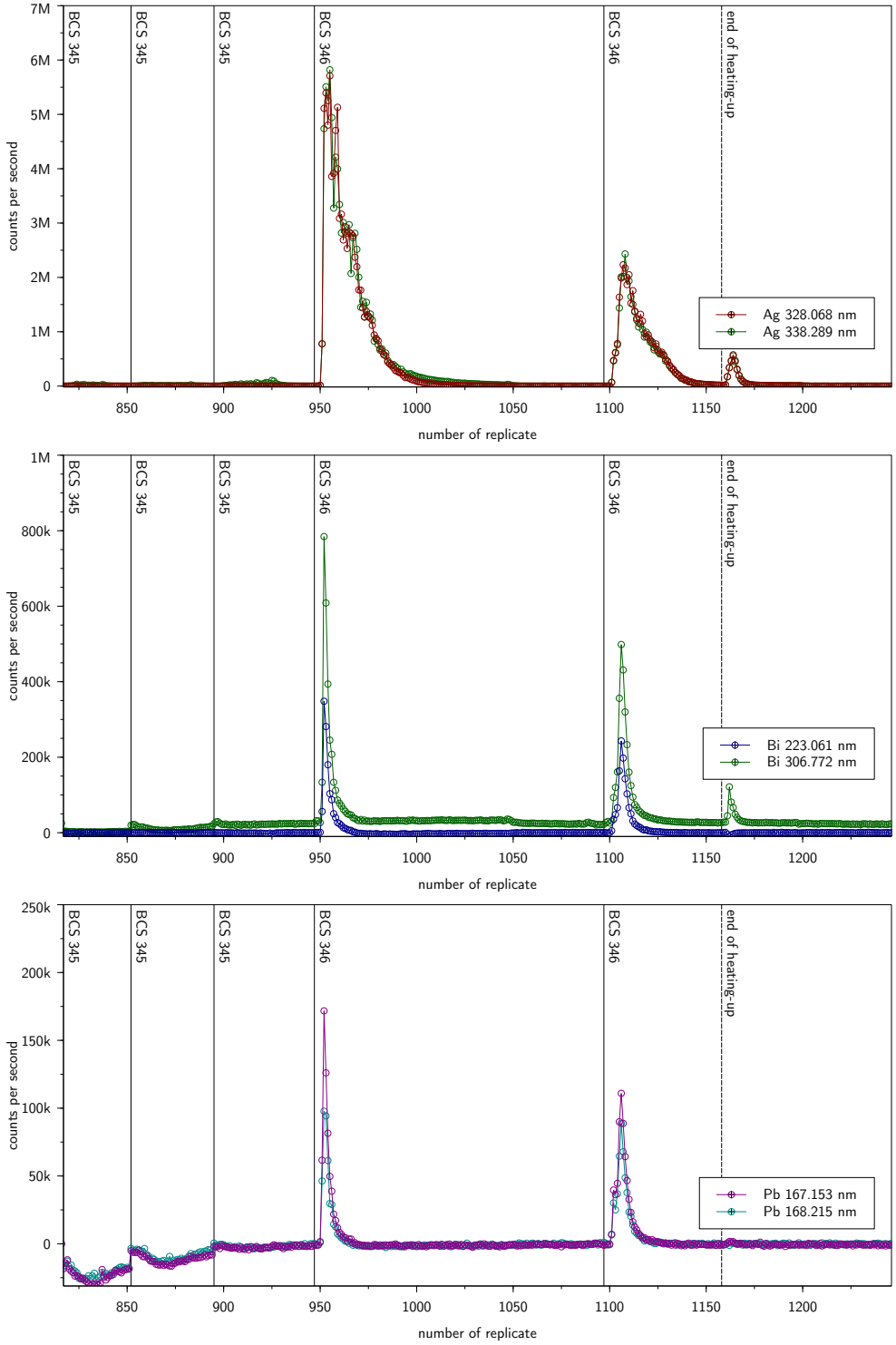

Figure 3.7.: Three times BCS 345 and two times BCS 346 heated up in a row on the same boat

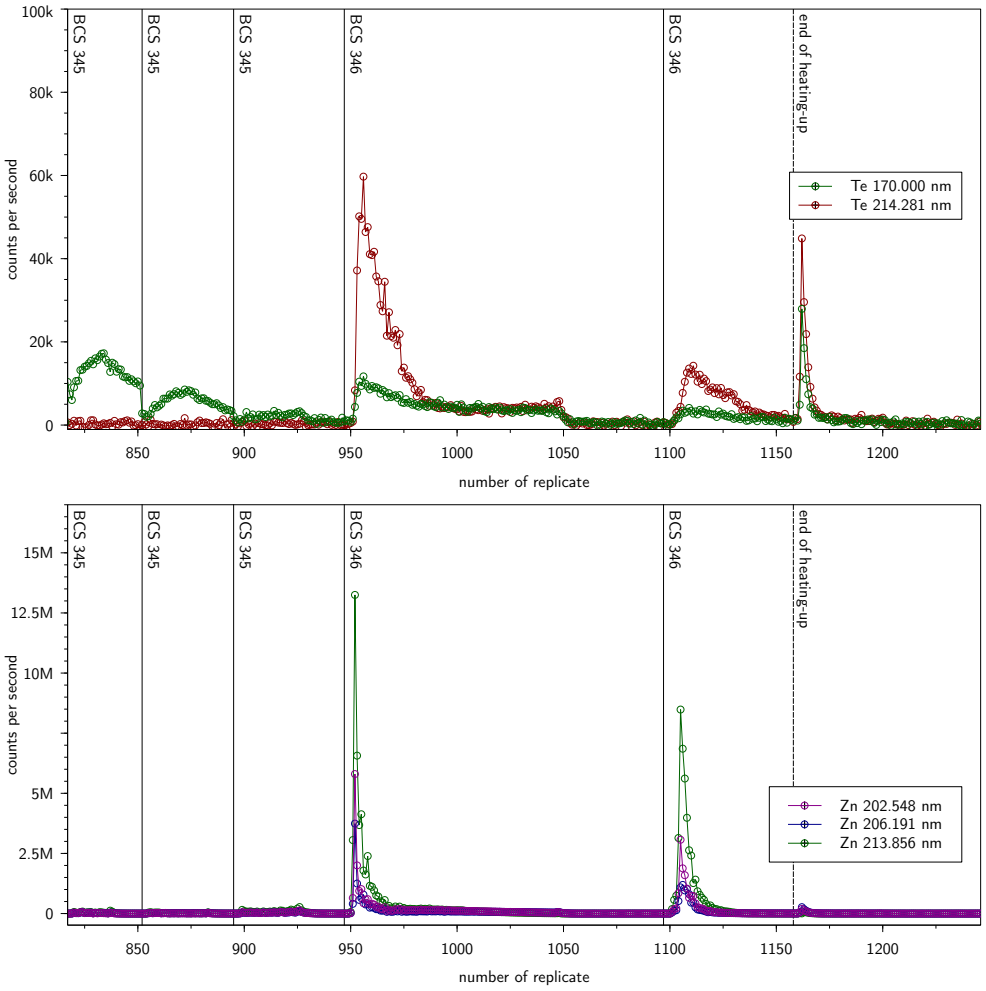

Figure 3.7.: Three times BCS 345 and two times BCS 346 heated up in a row on the same boat (continued)

CHAPTER 4

Conclusion

This last chapter summarizes the results and knowledge gained from working on this project. Admittedly, there was not sufficient time to investigate the concept of the TBF more thoroughly but it is thought that even the sparse results serve as a proof of concept.

4.1. Preliminary Results

Although not very extensive the results mentioned above nevertheless show that it is possible to vaporize certain analytes like silver, bismuth, lead, tellurium and zinc from a steel sample using direct solid sampling and a TBF. Care must be taken to choose the right emission lines for each element as to avoid interference from the line-rich tungsten spectrum and/or potentially the spectra of the matrix. The peak profile seems to depend roughly on the boiling temperatures of the corresponding elements, becoming broader with increasing T_b and limiting the analyzable elements to the easily volatile ones. As expected the sensitivity of this technique seems to be extraordinarily high eventually enabling analysis of ultra traces within steel samples. Regarding LODs so far the results are comparable to LA [11] but considering the costs of a fs-laser and an ICP-MS the combination of a TBF with (an mostly already available) ICP-OES seems far more suitable for routine analysis, not to mention ease of use. Another fact is that the LODs in this work were determined for a sample weight in the range of 30 mg, but supposedly the TBF can be loaded with much higher sample masses (as

demonstrated in a preceding experiment), potentially further lowering the detection limits by a factor of 5-10.

Altogether the results indicate that the determination of certain elements by TBF measurement is possible. Evidently further investigation is necessary for each analyte of interest in order to identify interferences and proper vaporization settings, empowering the technique to actually get valid values.

4.2. Remaining Issues

Because of the rather high temperatures required for analyte vaporization there is a significant amount of tungsten released into the plasma, leading to a high structured background. Controlling and reducing the current through the furnace and therefore the temperature of the boat could be useful to establish compromising conditions for rapid analyte evaporation and low tungsten or matrix release.

Furthermore, it was not possible to separate the remaining sample matrix from the boat. It appears that an intermetallic compound between the tungsten and the steel sample is formed. This in turn changes the thermal and resistive properties of the boat, making it difficult to achieve the same temperature in a second shot. Also the potential forming alloy presumably becomes softer and sometimes brittle, bearing the risk of cracking after using the boat for a longer time. To overcome this problem it was tried to add a separating layer between the tungsten and the steel sample. Ideally this layer would not melt, hinder the sample from touching the tungsten boat without shielding the sample too much from heat at the same time. So far this search has been unsuccessful.

In literature the use of a sample cuvette, made out of an identical tungsten boat by simply cutting of the ends, leaving only the dip for the sample, is described [2]. Such a cuvette can be placed on top of the heated boat containing the sample. After being used the sample residue can reportedly be removed by soaking the cuvette in hydrochloric acid over night, allowing the continuous use of the same tungsten boat over a long time period.

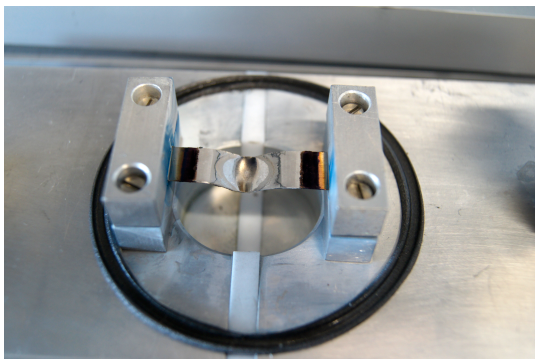

Figure 4.1.: Tungsten boat with oxides and steel sample melted together. The dark violet parts near the mounting blocks are composed of tungsten oxides, also note the blue oxide which has precipitated on the blocks directly while heating up. In the middle the silvery, shiny part is the remaining sample matrix alloyed with the tungsten. Also due to thermal expansion the dent facing downwards was created.

Figure 4.2.: Tungsten strips used for first experiments. Located on the left is the new strip while the one on the right has been fired several times containing steel samples. The remains are not separable of the tungsten anymore and its surface has become rather brittle. One can notice the well which developed due to thermal expansion, weakening during forming of the alloy and of course gravity. Also some tungsten oxide is visible near the ends of the strip where temperature is not high enough to evaporate it.

Another possibility would include trying to tilt the boat while the steel sample is still molten. Maybe the major part could be poured out leaving only a small layer which hopefully does not disturb the heating process too much. As shown before no further analyte evaporation occurs at a later time. Clearly, the downside of this approach is a more complicated and demanding furnace construction.

Some peak profiles are accompanied by a few values of rather high intensity, not quite fitting into the general progression of the signal. During evaporation the sudden break-up of sample particles can lead to a temporary increase in analyte signal. At the end of the heating process this is possibly caused by variations of plasma conditions due to irregular gas flow (refer to figures 3.4c and 3.5). In order to clarify this completely it would be necessary to monitor both an argon and a tungsten line as irregularities should be reflected in the signal of either one of these.

Generally all of the operating conditions should be controlled more accurately which would need a partially new design of the furnace and its power supply. Then further investigation of evaporation characteristics of individual elements as well as line selection and interference identification should be performed in order to improve usability and analytical figures of merit of the TBF.

In conclusion it was shown that the use of a TBF as an ETV device combined with ICP-OES provides an appealing method for solid sampling of steel. The increased sensitivity bears a route to analyzing very low analyte contents, together with rapid sample preparation and short measurement times a technique suitable for routine analysis is envisioned.

List of Figures

List of Tables

Bibliography

[1] Chemical Rubber Company, ed. *CRC Handbook of Chemistry and Physics*. 58th ed. Taylor and Francis, 1977.

[2] Hiroko Kataoka et al. „Magnetic Drop-In Tungsten Boat Furnace Vaporisation Inductively Coupled Plasma Atomic Emission Spectrometry (MDI-TBF-ICP-AES) for the Direct Solid Sampling of Iron and Steel“. *J. Anal. At. Spectrom.* 23 (2008), pp. 1108–1111.

[3] Erik Lassner and Wolf-Dieter Schubert. *Tungsten: Properties, Chemistry, Technology of the Element, Alloys, and Chemical Compounds*. 1st ed. Springer, Berlin, 1999.

[4] Henry P. Longerich, Simon E. Jackson, and Detlef Günther. „Laser Ablation Inductively Coupled Plasma Mass Spectrometric Transient Signal Data Acquisition and Analyte Concentration Calculation“. *J. Anal. At. Spectrom.* 11 (1996), pp. 899–904.

[5] Yoshisuke Nakamura et al. „Evaluation of Electrothermal Vaporization, Emission Intensity-Time-Wavelength Measurement and Time Resolution Combined With an Axially Viewed Horizontal Inductively Coupled Plasma Using an Echelle Spectrometer With Wavelength Modulation“. *J. Anal. At. Spectrom.* 12 (1997), pp. 349–354.

[6] Yasuaki Okamoto et al. „Determination of Vanadium and Titanium in Steel by Inductively Coupled Plasma Atomic Emission Spectrometry with Modified Use of a Tungsten Boat Furnace Atomizer for Atomic Absorptio Spectrometry“. *Anal. Chim. Acta* 239 (1990), pp. 139–143.

[7] Yasuaki Okamoto et al. „Direct Determination of Bismuth in Steel Samples by Magnetic Drop-In Electrothermal Vaporization Inductively Coupled Plasma Atomic Emission Spectrometry“. *J. Appl. Spectrosc.* 63, 12 (2009), pp. 1403–1406.

[8] E. R. Plante and A. B. Sessoms. „Vapor Pressure and Heat of Sublimation of Tungsten“. *Journal of Research of the National Bureau of Standards* 77A, 2 (1973), pp. 237–242.

[9] Yu. Ralchenko, A. Kramida, and J. Reader. *NIST Atomic Spectra Database (Version 4.1)*. May 2012. URL: `http://physics.nist.gov/asd`.

[10] Bernhard Welz and Michael Sperling. *Atomabsorptionsspektrometrie*. 4th ed. Wiley-VCH, 1997.

[11] Helmar Wiltsche and Detlef Günther. „Capabilities of Femtosecond Laser Ablation ICP-MS for the Major, Minor, and Trace Element Analysis of High Alloyed Steels and Super Alloys“. *Anal. Bioanal. Chem.* 399, 6 (2011), pp. 2167–2174.

[12] Helmar Wiltsche et al. „Characterization of a Multimode Sample Introduction System (MSIS) for Multielement Analysis of Trace Elements in High Alloy Steels and Nickel Alloys Using Axially Viewed Hydride Generation ICP-AES“. *J. Anal. At. Spectrom.* 23 (2008), pp. 1253–1262.

[13] Helmar Wiltsche et al. „Simultaneous Determination of As, Bi, Se, Sn and Te in High Alloy Steels - Re-evaluation of Hydride Generation Inductively Coupled Plasma Atomic Emission Spectrometry“. *J. Anal. At. Spectrom.* 22 (2007), pp. 1083–1088.

Acronyms

AAS atomic absorption spectrometry. 1, 3–6, 13, 69
AC alternating current. 22
ADC analog-digital converter. 27, 31
AES atomic emission spectrometry. 4, 69

CCD charge-coupled device. 37, 38
CRM certified reference material. 35, 38, 39, 45, 54, 59

DAC digital-analog converter. 27, 29, 31
DC direct current. 21, 22

EEPROM electrically erasable programmable read-only memory. 29, 30
ETV electrothermal-vaporization. 1, 2, 10–12, 68

FET field effect transistor. 23–25
FWHM full width at half maximum. 3

GF graphite furnace. 1, 6, 8, 22
GUI graphical user interface. 29, 31, 32

HCL hollow cathode lamp. 4, 5
HDR high dynamic range. 37

IC integrated circuit. 23–25, 27
ICP inductively-coupled plasma. 5–7, 69
ICP-MS inductively-coupled plasma mass spectrometry/spectrometer. 65
ICP-OES inductively-coupled plasma optical emission spectrometry/spectrometer. 1–3, 9, 13, 17, 19, 35–37, 65, 68, 71

LA laser ablation. 58, 59, 65

LOD limit of detection. 10, 35, 39, 56, 58, 59, 65

MOSFET metal oxide semiconductor field effect transistor. 22–25

PC personal computer. 27, 32
PCB printed circuit board. 23
PMT photomultiplier tube. 8, 9, 38
PTFE polytetrafluorethylene. 18
PVC polyvinylchloride. 18, 78
PWM pulse width modulation. 24–27, 69

RF radiofrequency. 6, 36

SNR signal-to-noise ratio. 8, 37, 53–55
SPS switching power supply. 20–22, 29, 71

TBF tungsten boat furnace. 1, 2, 8, 17, 18, 22, 27, 28, 31, 32, 35, 65, 66, 68

UART universal asynchronous receiver/transmitter. 27
USB universal serial bus. 27

APPENDIX A

Blueprints

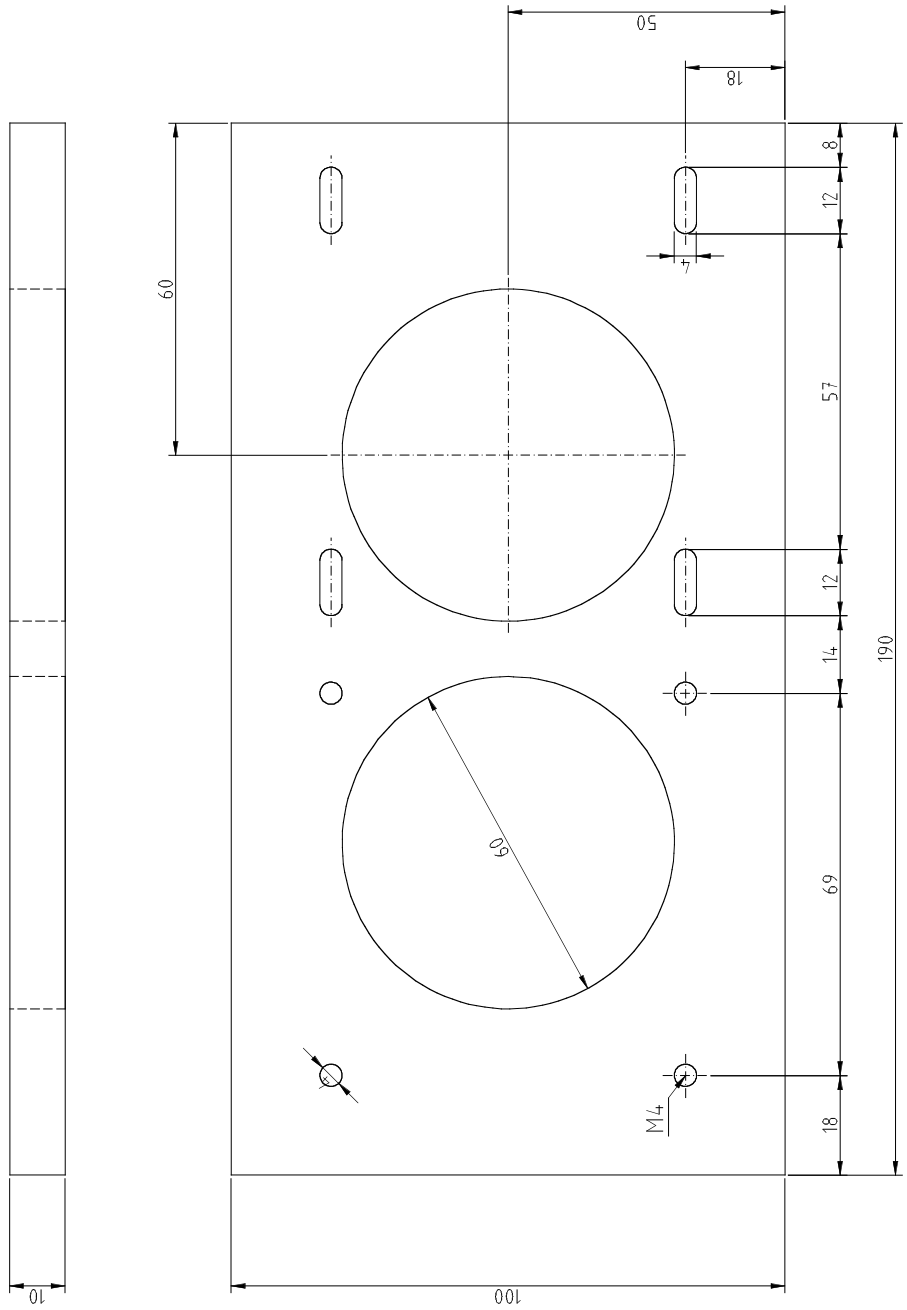

Figure A.1.: Base plate (PVC)

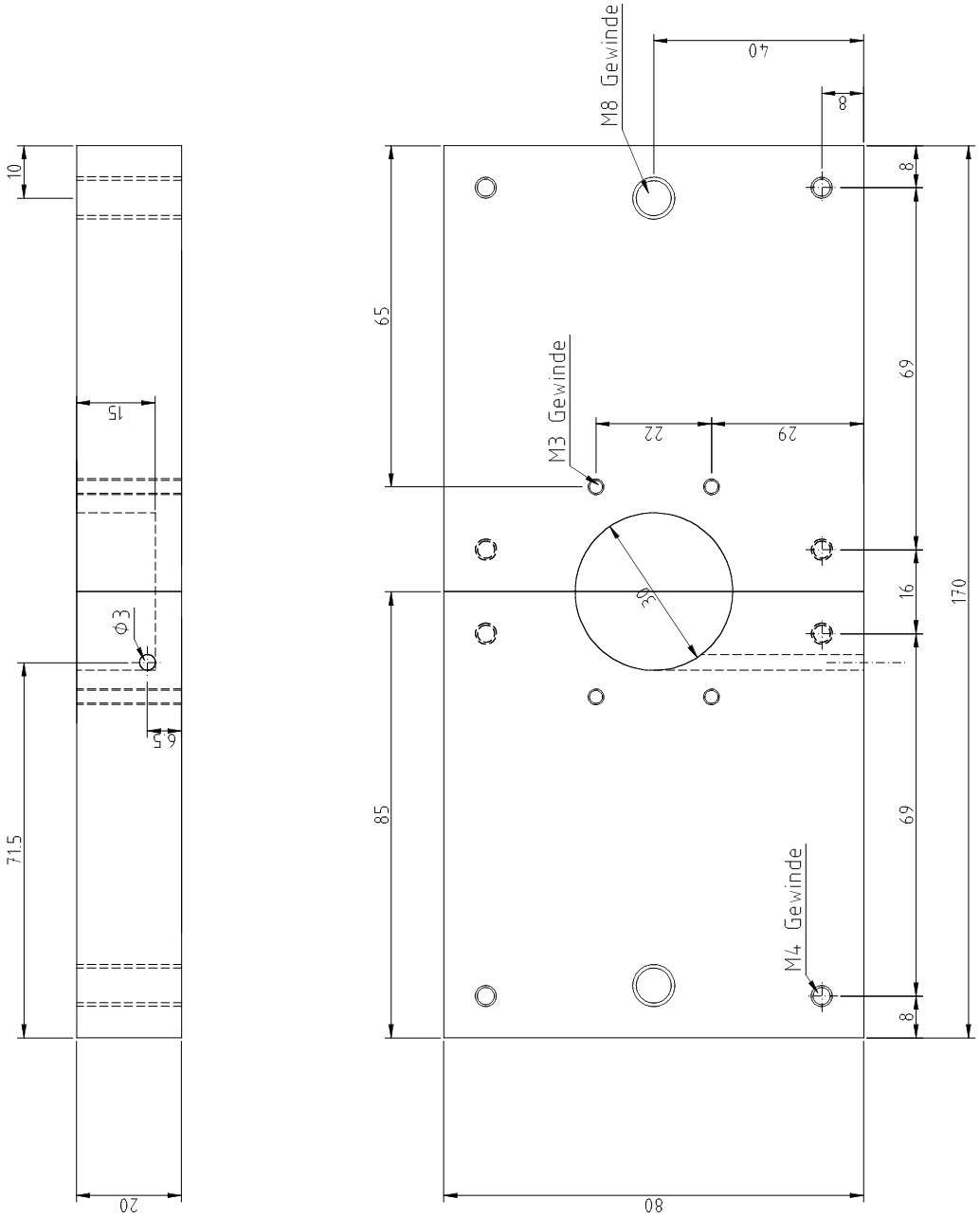

Figure A.2.: Electrode blocks (aluminium)